

The Surprising Effectiveness of MAPPO in Cooperative, Multi-Agent Games

Chao Yu ^{*1} Akash Velu ^{*2} Eugene Vinitsky ^{†2} Yu Wang ¹ Alexandre Bayen ² Yi Wu ^{†13}

yc19@mails.tsinghua.edu.cn, akashvelu@berkeley.edu, evinitsky@berkeley.edu, yu-wang@tsinghua.edu.cn, director-its@berkeley.edu, jxwuyi@gmail.com

Abstract

Proximal Policy Optimization (PPO) is a popular on-policy reinforcement learning algorithm but is significantly less utilized than off-policy learning algorithms in multi-agent problems. In this work, we investigate Multi-Agent PPO (MAPPO), a multi-agent PPO variant which adopts a centralized value function. Using a 1-GPU desktop, we show that MAPPO achieves performance comparable to the state-of-the-art in three popular multi-agent testbeds: the Particle World environments, Starcraft II Micromanagement Tasks, and the Hanabi Challenge, with minimal hyperparameter tuning and without any domain-specific algorithmic modifications or architectures. In the majority of environments, we find that compared to off-policy baselines, MAPPO achieves better or comparable sample complexity as well as substantially faster running time. Finally, we present 5 factors most influential to MAPPO’s practical performance with ablation studies.

1. Introduction

With recent advances in deep reinforcement learning (RL), we have witnessed many achievements in building intelligent agents to solve complex multi-agent challenges: AlphaStar achieved top professional-player level performance in Starcraft II (Vinyals et al., 2019), OpenAI Five defeated the world champion in Dota II (Berner et al., 2019), and RL was even used to demonstrate emergent, human-like tool-use in a simulated physical world (Baker et al., 2020).

These successes were accomplished using distributed on-policy RL algorithms such as IMPALA (Espeholt et al., 2018) and PPO (Schulman et al., 2017) but required massive amounts of parallelism and compute; tens of thousands of CPU cores and tens or hundreds of GPUs were utilized

^{*}Equal contribution, [†]Equal advising ¹Tsinghua University ²UC Berkeley ³Shanghai Qi Zhi Institute. Correspondence to: Akash Velu <akashvelu@berkeley.edu>, Yi Wu <jxwuyi@gmail.com>.

to collect and train on an extraordinary volume of training samples. Consequently, it has almost become a domain consensus that on-policy RL algorithms such as PPO are much less sample efficient than off-policy learning algorithms, and may not be suitable in academic settings with limited computational resources. Hence, recent multi-agent reinforcement learning (MARL) literature has primarily adopted off-policy learning frameworks, such as MADDPG (Lowe et al., 2017) and value-decomposed Q-learning (Sunehag et al., 2018; Rashid et al., 2018). A variety of algorithmic variants with domain-specific modifications have been proposed within this framework, producing state-of-the-art (SOTA) results on a wide range of multi-agent benchmarks (Hu & Foerster, 2020; Wang et al., 2021).

In this paper, we re-examine this sample-efficiency hypothesis by carefully evaluating an on-policy MARL algorithm, Multi-Agent PPO (MAPPO), a multi-agent PPO variant using a centralized value function, on three popular MARL testbeds: the multi-agent particle-world environment (MPE) (Lowe et al., 2017), the Starcraft micromanagement challenge (SMAC) (Rashid et al., 2019), and the Hanabi challenge (Bard et al., 2020). We focus on fully cooperative tasks in order to compare our results directly with the performance of state-of-the-art (SOTA) agents. Additionally, we only utilize a single desktop machine with 1 GPU and 1 multicore CPU for training.

Surprisingly, even with these limited computational resources, MAPPO performs comparably to SOTA on all test scenarios, including 3 cooperative MPE tasks, the 23 SMAC maps, and the full-scale Hanabi game. Importantly, we observe that compared to other off-policy MARL algorithms, MAPPO consistently has a substantially faster run-time and comparable or even improved *sample complexity*. We also conduct ablation studies on the factors most influential to MAPPO’s practical performance and provide five concrete implementation suggestions, which, to the best of our knowledge, have not yet attracted sufficient attention in the existing literature.

Our contributions are summarized as follows:

- We show that Multi-Agent PPO (MAPPO), with minimal hyper-parameter tuning and without any domain-

specific algorithmic changes or architectures, achieves performances comparable to SOTA on 3 benchmarks.

- We demonstrate MAPPO achieves significantly faster run-time and comparable sample complexity to off-policy MARL methods, using a 1-GPU desktop.
- We suggest 5 implementation factors that govern the practical performance of MAPPO and release our source code at <https://sites.google.com/view/mappo>.

2. Related Work

MARL algorithms can be categorized into two frameworks: centralized and decentralized learning. Centralized methods (Claus & Boutilier, 1998) assume a cooperative game (Panait & Luke, 2005) and directly extend single-agent RL algorithms by learning a single policy to produce the joint actions of all agents simultaneously. In decentralized learning (Littman, 1994), each agent optimizes its own reward independently; these methods can tackle general-sum games but may suffer from non-stationary transitions. Recent work has developed two lines of research to bridge the gap between these two frameworks: *centralized training and decentralized execution (CTDE)* and *value decomposition (VD)*. CTDE improves upon decentralized RL by adopting an actor-critic structure and learning a centralized critic for variance reduction. Representative CTDE methods include MADDPG (Lowe et al., 2017) and COMA (Foerster et al., 2018). VD is typically combined with centralized Q-learning by representing the joint Q-function as a function of each agent’s local Q-function (Sunehag et al., 2018; Rashid et al., 2018; Son et al., 2019), which has been considered as the gold standard for many MARL benchmarks. Our method, MAPPO, falls into the CTDE category by combining individual PPO training with a global value function.

Early works (Duan et al., 2016) suggested that the on-policy RL algorithm TRPO outperforms the off-policy algorithm DDPG in continuous control tasks. However, recent advances in off-policy methods, such as SAC (Haarnoja et al., 2018) and Rainbow (Hessel et al., 2018), have led to a new consensus that even the latest policy gradient (PG) algorithms, such as PPO, are significantly less sample efficient than their off-policy competitors. In many single-agent domains, including MuJoCo control (Stooke & Abbeel, 2019), Atari games (Dhariwal et al., 2017), and real robot systems (Mahmood et al., 2018), off-policy methods currently are state-of-the-art in terms of sample complexity. Similar conclusions have also been drawn in multi-agent domains. Papoudakis et al. (2020) report that multi-agent PG methods, e.g., COMA, are outperformed by MADDPG and QMix (Rashid et al., 2018) by a clear margin in both the multi-agent particle-world environment (MPE) (Mordatch & Abbeel, 2017) and the Starcraft II Micromanagement challenge (SMAC) (Rashid et al., 2019). Hu & Foerster (2020) achieve SOTA in the Hanabi challenge (Hanabi) (Bard et al.,

2020) with a domain-specific Q-learning variant. Note that although de Witt et al. (2020) empirically notice that fully decentralized independent PPO training (IPPO) can achieve surprisingly high success rates on some specific hard SMAC maps, the cause for this success is unknown, and the overall performance of IPPO remains much worse than QMix. We re-examine these conclusions about PPO and show that MAPPO is able to achieve SOTA performance on 3 popular cooperative MARL testbeds.

Many existing works have studied the implementation details of policy gradient algorithms in the single-agent continuous control domain. Tucker et al. (2018) point out that advantage normalization is critical for the practical use of PG. Ilyas et al. (2020) analyze the accuracy of the estimated gradients and suggest the usage of large batch sizes to reduce the high variance of PG. Engstrom et al. (2020) examine the code level implementation details that are most impactful to PPO’s improved performance over TRPO; similarly, Andrychowicz et al. (2021) investigate the effect of PPO’s hyperparameters and provide concrete tuning suggestions.

We consider multi-agent games and investigate factors that are either largely ignored in the existing literature or are completely unique to the multi-agent setting. Although our multi-agent benchmarks have significantly different dynamics from single-agent environments such as MuJoCo, we do find a few previous suggestions, such as input normalization, value clipping, orthogonal initialization, and gradient clipping, to be helpful and include them in our implementation. Liu et al. (2019) suggest that regularization can positively impact RL training, which is consistent with our practice of using layer normalization. Lastly, Hsu et al. (2020) suggest using a soft trust-region penalty and discretizing the action space for PPO to avoid bad local optima in continuous control domains, which is consistent with the improved performance we see in the discrete tasks we consider.

3. Preliminaries

We study decentralized partially observed Markov decision processes (DEC-POMDP) (Oliehoek et al., 2016) with shared rewards. A DEC-POMDP is defined by $\langle \mathcal{S}, \mathcal{A}, \mathcal{O}, R, P, n, \gamma \rangle$. \mathcal{S} is the state space. \mathcal{A} is the shared action space for each agent. $o_i = \mathcal{O}(s; i)$ is the local observation for agent i at global state s . $P(s'|s, A)$ denotes the transition probability from S to S' given the joint action $A = (a_1, \dots, a_n)$ for all n agents. $R(s, A)$ denotes the shared reward function for each agent. γ is the discount factor. We follow the centralized-training-decentralized-execution framework with parameter sharing, where each agent uses a shared policy $\pi_\theta(a_i|o_i)$ parameterized by θ to produce its action a_i from its local observation o_i , and optimizes its discounted accumulated reward $J(\theta) = \mathbb{E}_{a^t, s^t} [\sum_t \gamma^t R(s^t, a^t)]$.

4. Multi-Agent PPO (MAPPO)

We adapt the single-agent PPO algorithm to the multi-agent setting by learning a policy π_θ and a centralized value function $V_\phi(s)$ based on a global state s instead of the local observation o_i . We maintain two separate networks for the policy π_θ and the value function V_ϕ and follow common practices in PPO implementation, including: *Generalized Advantage Estimation (GAE)* (Schulman et al., 2016) with advantage normalization, observation normalization, gradient clipping, value clipping, layer normalization, ReLU activation with orthogonal initialization, and a large batch size under our 1-GPU constraint. Pseudocode and algorithmic details can be found in Appendix D. We also perform a limited grid-search over certain hyper-parameters, including network architecture (i.e., whether to use an MLP network or a recurrent network), learning rate, entropy bonus coefficient, and the initialization scale of the final layer in the policy network. Full details can be found in Appendix D.1.

We additionally present 5 concrete implementation suggestions that we find to be particularly critical to MAPPO’s practical performance: value normalization, agent-specific global state, training data usage, action masking, and death masking. Empirical studies can be found in Section 6.

4.1. Value Normalization

To stabilize value learning, we follow the PopArt technique proposed by Hessel et al. (2019) and normalize the values by a running average over the value estimates. Concretely, during value learning, the value network will regress to the normalized target values. When computing the GAE, we will use the running average to denormalize the output of the value network so that the value outputs are properly scaled. We find that using PopArt never hurts training and often significantly improves the final performance of MAPPO.

Suggestion 1: Always use PopArt value normalization.

4.2. Agent-Specific Global State

Conceptually, the input to the value network is the only fundamental difference between multi-agent PG algorithms and fully decentralized PG. Therefore, the representation of the value input becomes critical to the overall algorithm. The underlying assumption of centralized value functions is that observing the full global state reduces a POMDP to an MDP and therefore makes value learning much easier. An accurate value function further improves policy learning.

There are two common practices. Lowe et al. (2017) propose to use the concatenation of all local observations, i.e., (o_1, \dots, o_n) , as the input to the critic. This method is generic but can pose problems when n is large or the dimension of o_i is high — in this case, the input dimension of the value network becomes significantly higher than the

policy network, which makes value learning substantially more challenging. In turn, an inaccurate value function further hurts policy learning. An alternate approach is to use the global information provided by the environment. For example, the SMAC environment provides a vector containing information about all agents and enemies, which has been widely adopted as the global state representation in most existing SMAC experiments. However, we remark that an improperly chosen approximate global state may even contain *less* information than a local observation, which can again make value learning harder.

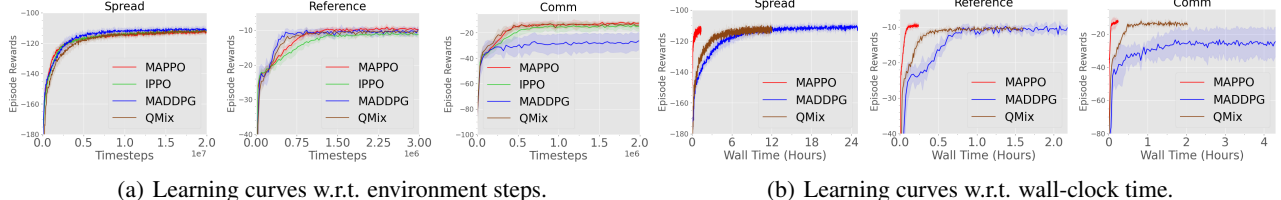
Specifically, we notice that although local observations in the SMAC environment lack information about out of sight allies and enemies, they do contain many agent-specific features, such as agent id, available actions, and relative distances to all enemies and teammates, that are not in the global state. We hypothesize that the loss of essential local features in the global state is an important factor in yielding the results reported in (de Witt et al., 2020) that fully decentralized PPO, learning purely on local observations, can sometimes be better than centralized PPO.

Therefore, we propose to use a value network input that is an agent-specific global state which contains all global information and the necessary agent-specific features. Specifically for the SMAC environment, we implement a customized function to compute an augmented global state that includes all invisible enemy and agent information while keeping agent-specific features. We remark that an agent-specific global cannot be used in QMix, which uses a single mixer network common to all agents.

Suggestion 2: Include agent-specific features in the global state and check that these features do not make the state dimension substantially higher.

4.3. Training Data Usage

PPO uses importance sampling to perform off-policy corrections, allowing for sample reuse. After a batch of samples is collected, Schulman et al. (2017) suggest splitting the large batch into mini-batches and training over this batch for multiple epochs. In continuous control domains, the common practice is to train for tens of epochs with around 64 mini-batches per epoch. However, we find that in multi-agent domains, MAPPO’s performance degrades when samples are re-used too often, perhaps as a consequence of non-stationarity in the environment. Thus, we use 15 epochs for easy tasks, and 10 or 5 epochs for difficult tasks. Furthermore, similar to the suggestions by (Ilyas et al., 2020), we always find that using more data to estimate gradients leads to improved practical performance; thus, we do not split training data into mini-batches by default. We find that avoiding minibatching is useful in all but one SMAC map, in which splitting the training batch into two mini-



(a) Learning curves w.r.t. environment steps.

(b) Learning curves w.r.t. wall-clock time.

Figure 1. Sample efficiency and wall clock time of different algorithms in MPE.

batches improves performance. We hypothesize that mini-batching in this scenario helps escape a poor local optimum, similar to phenomena observed in the supervised learning setting (Kleinberg et al., 2018).

Suggestion 3: Avoid using too many training epochs and do not split data into mini-batches by default.

4.4. Action Masking

In multi-agent games, it is often the case that some actions cannot be executed due to game constraints. For example, in SMAC, an agent may have skills that cannot be performed frequently; in Hanabi, each player can only perform specific actions when they have enough tokens left. So, when computing the logits for the softmax action probability $\pi_\theta(a_t|o_t)$, we mask out the unavailable actions in both the forward and backward pass so that the probabilities for unavailable actions are always zero. We find that this substantially accelerates training.

Suggestion 4: Mask out unavailable actions when computing action probabilities.

4.5. Death Masking

In multi-agent games, an agent may die before the game terminates (e.g., SMAC). Note that we can always access the game state to compute the agent-specific global state for those dead agents. Therefore, even if an agent dies and becomes inactive in the middle of a rollout, value learning can still be performed in the following timesteps using inputs containing information of other live agents. This is typical in many existing multi-agent PG implementations.

However, we argue that using these informative states for dead agents during value learning amplifies the bias of the learned value function. Consequently, high value prediction errors in timesteps at which the agent is dead will be accumulated during the GAE computation, in turn hindering policy learning over the timesteps in which the agent is still alive. Our suggestion is to simply use an agent-specific constant vector, i.e., a zero vector with the agent’s ID, as the input to the value function after an agent dies. We call this approach “Death Masking”. Further justifications for this method are provided in Appendix B.

Suggestion 5: Use zero states with agent ID as the value input for dead agents.

5. Main Results

In this section, we compare MAPPO with other MARL algorithms on the multi-agent particle-world environment (MPE), the Starcraft micromanagement challenge (SMAC), and the Hanabi challenge (Hanabi). Baseline comparison methods include MADDPG, QMix, and fully decentralized PPO (IPPO), which uses local observations as the value input, but otherwise follows all of the previously mentioned PPO implementation suggestions. For a fair comparison, we ensure that all baseline methods use the same implementation practice and adopt the same hyper-parameter tuning process as MAPPO (more details are in Appendix D.1). We emphasize that our reported numbers for the baselines in this paper *all match or exceed those in the original papers*. Furthermore, we compare MAPPO with the SOTA methods for each domain, namely RODE (Wang et al., 2021) on SMAC and SAD (Hu & Foerster, 2020) on Hanabi. All SOTA numbers for these two algorithms are obtained from their original papers.

Each experiment is performed on a desktop machine with 256 GB RAM, one 64-core CPU, and one GeForce RTX 3090 GPU, which is used for forward action computation and training updates. To compute wall-clock time, MAPPO runs 128 parallel environments in MPE and 8 in SMAC while the off-policy algorithms use a single environment, which is consistent with the implementation used in the original papers. Due to limited machine resources, we use at most 5 GB GPU memory for SMAC experiments and 13 GB GPU memory for Hanabi. More environment and implementation details can be found in Appendix C and D.1.

Empirical Findings: we observe that in the vast majority of environments, MAPPO achieves results better or comparable to SOTA with **comparable or better sample complexity** and **substantially faster wall-clock training time**.

5.1. MPE Results

We consider the 3 cooperative tasks originally proposed in (Lowe et al., 2017), including the physical deception task (*Spread*), the simple reference task (*Reference*), and the cooperative communication task (*Comm*), and compare MAPPO with MADDPG, IPPO and QMix. As the observation dimensions in the MPEs are low, we use a concatenation of all local observations as the global state. The performance

The Surprising Effectiveness of MAPPO in Cooperative, Multi-Agent Games

| Maps | Difficulty | MAPPO | IPPO | QMIX | RODE | MAPPO(cut) | QMIX(cut) |
|------------------|------------|-------------------|-------------------|-------------------|--------------------|------------|------------|
| 2m vs. 1z | Easy | 100.0(0.0) | 100.0(0.0) | 95.3(5.2) | / | 100.0(0.0) | 100.0(2.9) |
| 3m | Easy | 100.0(0.0) | 100.0(0.0) | 96.9(1.3) | / | 100.0(0.0) | 93.8(1.9) |
| 2s vs. 1sc | Easy | 100.0(0.0) | 100.0(1.5) | 96.9(2.9) | 100(0.0) | 100.0(0.0) | 96.9(0.7) |
| 2s3z | Easy | 100.0(0.7) | 100.0(0.0) | 95.3(2.5) | 100(0.0) | 100.0(1.5) | 92.2(3.9) |
| 3s vs. 3z | Easy | 100.0(0.0) | 100.0(0.0) | 96.9(12.5) | / | 100.0(0.0) | 100.0(1.5) |
| 3s vs. 4z | Easy | 100.0(0.9) | 100.0(0.0) | 97.7(1.9) | / | 100.0(1.9) | 84.4(3.7) |
| so many baneling | Easy | 100.0(0.0) | 100.0(1.5) | 96.9(2.3) | / | 100.0(1.5) | 81.2(2.6) |
| 8m | Easy | 100.0(0.0) | 100.0(0.7) | 97.7(1.9) | / | 100.0(0.0) | 93.8(2.7) |
| MMM | Easy | 96.9(2.6) | 96.9(0.0) | 95.3(2.5) | / | 93.8(2.6) | 92.2(3.9) |
| 1c3s5z | Easy | 100.0(0.0) | 100.0(0.0) | 96.1(1.7) | 100(0.0) | 100.0(0.0) | 95.3(1.5) |
| bane vs. bane | Easy | 100.0(0.0) | 100.0(0.0) | 100.0(0.9) | 100(46.4) | 100.0(0.0) | 100.0(0.0) |
| 3s vs. 5z | Hard | 96.9(37.5) | 97.7(1.7) | 98.4(2.4) | 78.9(4.2) | 96.9(41.7) | 56.2(6.4) |
| 2c vs. 64zg | Hard | 100.0(0.0) | 98.4(1.3) | 92.2(4.0) | 100(0.0) | 96.9(2.5) | 71.9(3.9) |
| 8m vs. 9m | Hard | 87.5(4.0) | 89.8(4.5) | 92.2(2.0) | / | 78.1(15.1) | 89.1(1.9) |
| 25m | Hard | 100.0(1.5) | 100.0(0.0) | 90.6(3.8) | / | 98.4(3.3) | 89.1(3.9) |
| 5m vs. 6m | Hard | 75.0(18.2) | 57.0(15.6) | 75.0(6.9) | 71.1(9.2) | 29.7(16.3) | 54.7(2.2) |
| 3s5z | Hard | 96.9(0.7) | 96.9(1.5) | 88.3(2.9) | 93.75(1.95) | 71.9(15.6) | 85.9(5.2) |
| 10m vs. 11m | Hard | 96.9(4.8) | 93.0(7.4) | 95.3(1.0) | 95.3(2.2) | 84.4(7.9) | 82.8(4.8) |
| MMM2 | Super Hard | 90.6(2.8) | 86.7(7.3) | 87.5(2.6) | 89.8(6.7) | 46.9(23.0) | 81.2(4.5) |
| 3s5z vs. 3s6z | Super Hard | 84.4(34.0) | 82.8(19.1) | 82.8(5.3) | 96.8(25.11) | 73.4(36.3) | 50.0(7.8) |
| 27m vs. 30m | Super Hard | 93.8(2.4) | 82.0(10.3) | 50.0(10.5) | 96.8(1.5) | 93.8(3.8) | 34.4(5.1) |
| 6h vs. 8z | Super Hard | 86.7(11.8) | 84.4(33.3) | 9.4(2.0) | 78.1(37.0) | 78.1(14.5) | 3.1(1.5) |
| corridor | Super Hard | 100.0(1.2) | 98.4(3.1) | 84.4(2.5) | 90.6(18.3) | 93.8(4.9) | 70.3(13.6) |

Table 1. Median evaluation win rate and standard deviation on all the SMAC maps for different methods, using at most 10M training timesteps. Columns with “cut” display results using the same number of timesteps as RODE.

of each algorithm at convergence is shown in Fig. 1(a). All results are averaged over 10 seeds. We observe that MAPPO achieves the highest rewards with the fewest amount of samples on all tasks. We additionally show the training reward w.r.t. the wall clock time of MADDPG, QMix, and MAPPO in Fig. 1(b). MAPPO is an order of magnitude faster than off-policy baselines since it takes fewer gradient updates.

5.2. SMAC Results

In SMAC, compare MAPPO with IPPO, QMix, and the SOTA algorithm, RODE (Wang et al., 2021), a domain-specific variant of QMix. We follow the evaluation metric proposed in (Wang et al., 2021): for each training seed, we compute the win rate over 32 test games after each training iteration and take the median of the final 10 evaluations as the performance for each training seed. We measure the median success rates over 6 seeds for all the methods in Table 1. The results for RODE are directly calculated using the released training and evaluation statistics from (Wang et al., 2021) while MAPPO, IPPO, and QMix are trained until convergence or reaching 10M environment steps. MAPPO has strong performance in the vast majority of SMAC maps and achieves the best win-rate in 19 of the 23 maps. Moreover, even in maps in which MAPPO does not produce SOTA performance, the gap between MAPPO and SOTA is

within 6.2%. The only exception is the 3s5z vs. 3s6z map, in which MAPPO does not converge after 10M steps but eventually reaches a 91% win-rate if run to convergence, as shown in Appendix E.1. In particular, MAPPO clearly outperforms QMix in the vast majority of maps, especially in the “super hard” maps. Compared to IPPO, MAPPO generally achieves superior performance and exhibits more stable training, suggesting that a centralized value function with an appropriate global state representation indeed improves upon decentralized learning.

Furthermore, since RODE uses fewer samples than our upper-limit of 10M steps, we report the performance of MAPPO and QMix using the same amount of samples as RODE in the rightmost columns of Table 1 (labeled “cut”). In this situation, despite being an on-policy algorithm and using a limited amount of samples, MAPPO outperforms QMix on 19/23 maps and achieves comparable performance to RODE. Although MAPPO is surpassed by RODE in the MMM2 and 5m vs. 6m maps, MAPPO notably exceeds RODE’s performance in Corridor and 3s vs. 5z.

In addition, we pick 5 representative maps and show the training curve of MAPPO, QMix, and RODE w.r.t. environment steps and wall-clock time in Fig. 2. It is clear that MAPPO achieves better or comparable sample complexity to the baselines while taking substantially less training time.

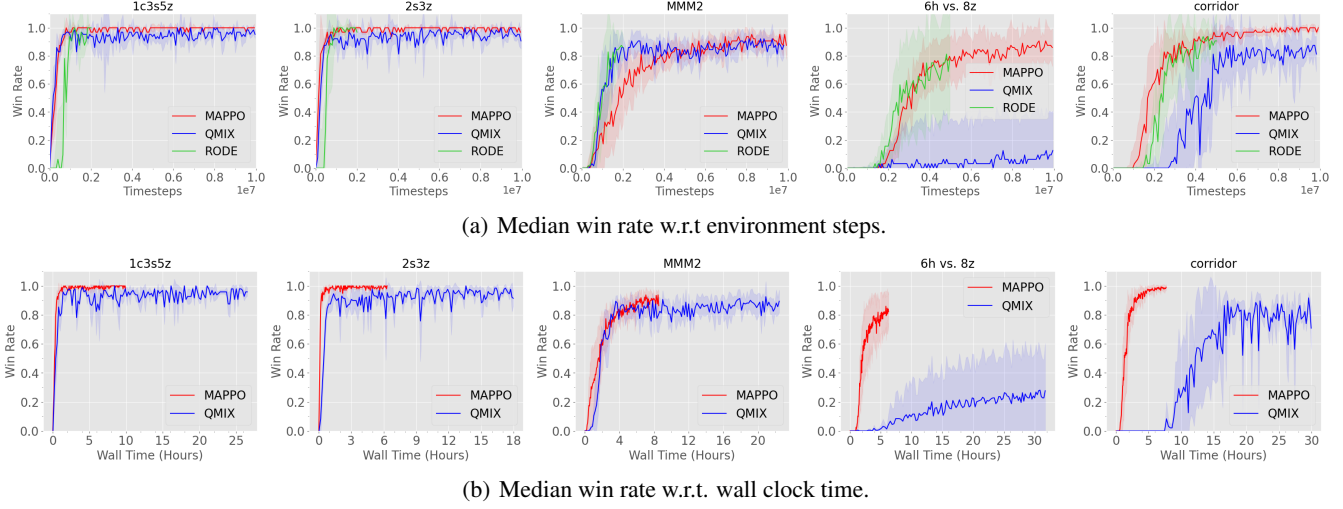


Figure 2. Sample efficiency and wall clock time of algorithms in SMAC.

The training curves for all the other maps can be found in Appendix E.1. We remark that despite MAPPO being less complex than RODE, it is able to achieve comparable final performance and sample complexity, suggesting that simple PPO-based algorithms are strong baselines in many multi-agent problems.

5.3. Hanabi Results

We evaluate MAPPO in the 2-player full-scale Hanabi game and compare with the SOTA result for model-free methods produced by SAD (Hu & Foerster, 2020), a Q-learning variant designed for the Hanabi game¹. For a fair comparison, we only compare to the SAD result trained without using auxiliary training tasks from (Hu & Foerster, 2020). Since Hanabi does not provide a global game state, we implement a function to compute a global-state by adding information about the agent’s own hand, which is not present in the agent’s local observation, into its global-state.

Note that SAD uses about 10B timesteps² and reports the best and average performance over 13 trials. Due to limited computational resources, we train MAPPO for only 7.2B environment steps over 4 random seeds. Each evaluation score is computed as an average over the scores obtained in 100k rollouts. Due to difficulties in code level optimizations, our implementation of MAPPO in Hanabi is not parallelized and so we do not report a wall-clock comparison for this problem.

The evaluation results are summarized in Table 2. Although it uses slightly fewer computational resources and training steps than SAD, MAPPO is still able to produce results close to both the best and average SOTA reward in the challenging

¹The overall SOTA score in 2 player Hanabi is 24.52, achieved by a search-based algorithm. (Hu et al., 2021)

²Reported in communication with authors

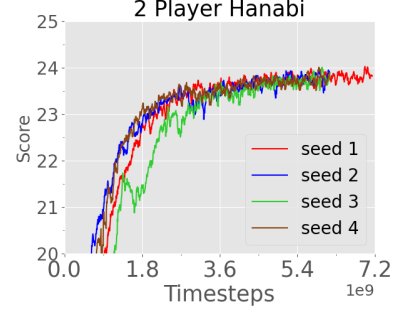


Figure 3. Score of MAPPO in 2-player Hanabi

| Algorithms. | Best | Average |
|-------------|-------|---------|
| SAD | 24.01 | 23.87 |
| MAPPO | 23.87 | 23.85 |

Table 2. Best and Average evaluation scores of MAPPO and SAD on Hanabi-Full with 2 players.

Hanabi game. As shown in Fig. 3, the results have not fully converged which suggests that the gap between MAPPO and SAD may close over the remaining 3 billion steps.

6. Ablation Studies on Suggestions

In this section, we examine the aspects of MAPPO which are most critical to its performance by presenting ablation studies of the 5 implementation suggestions described in Sec. 4: value normalization, agent-specific global state, training data usage, action masking, and death masking.

6.1. Value Normalization

We evaluate the performance of MAPPO with and without the value normalization described in Sec. 4.1 and display the evolution of average reward in the MPE *Spread* task and median win-rate in various SMAC maps in Fig. 4. We

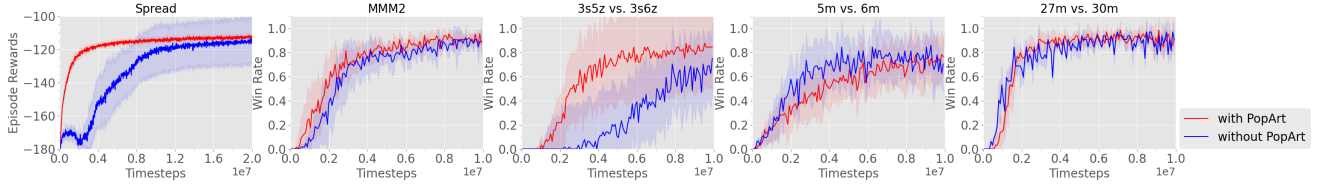


Figure 4. Ablation studies demonstrating the effect of value normalization on MAPPO’s performance in MPE and SMAC.

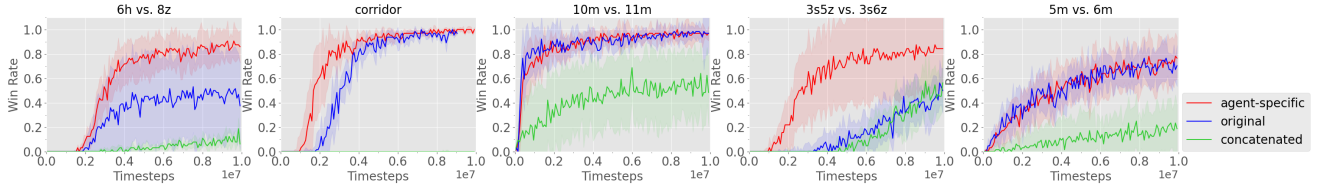


Figure 5. Ablation studies demonstrating the effect of global state on MAPPO’s performance in SMAC.

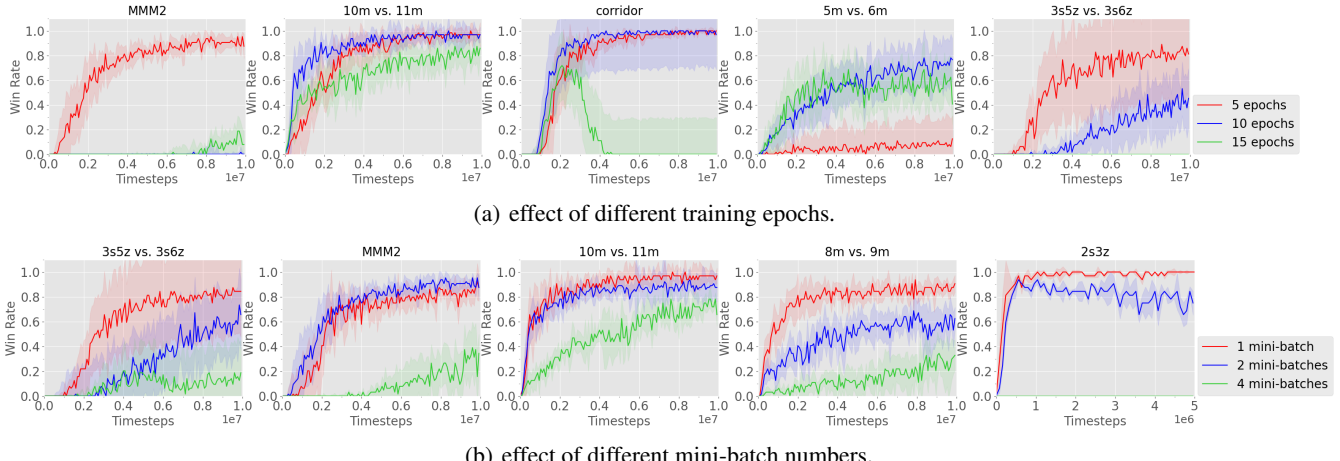


Figure 6. Ablation studies demonstrating the effect of epoch and mini-batch number on MAPPO’s performance in SMAC.

see that in *Spread*, where the episode rewards can range from below -200 to 0, value normalization is critical to performance. Value normalization also substantially benefits MAPPO’s performance in the *3s5z* vs. *3s6z* map. In other SMAC maps, value normalization does not improve the median performance, but does reduce the training variance, thus demonstrating its benefit to MAPPO’s performance.

6.2. Agent-Specific Global State

We compare our agent-specific global state representation (*agent-specific*) to two baselines in SMAC: (1) the original, agent-agnostic environment provided global state (*original*), and (2) the concatenation of all local agent observations (*concatenated*). The results in Fig. 5 demonstrate that using the *concatenated* global state, which is much higher dimensional than the *original* and *agent-specific*, is ineffective, particularly in maps with many agents. When using the *concatenated* global state, the presence of many agents leads to a very high state dimension which we conjecture harms training. In comparison, using the *original* environment global state achieves stronger results, but performs below par in difficult maps such as *6h* vs. *8z* and *3s5z* vs. *3s6z*. Using an *agent-specific* global state consistently results in

the strongest performance, showing that state dimensionality, agent-specific features, and global information are all important in forming an effective global state.

6.3. Training Data Usage

After a batch of episodes is collected, PPO updates both the actor and critic network through mini-batch gradient descent over multiple epochs. Although PPO’s importance sampling and clipping terms are specifically designed to enable high data reuse frequency, we find that MAPPO is particularly sensitive to data reuse in multi-agent settings.

We first examine the effect of training epochs in SMAC. Fig. 6(a) shows the performance of MAPPO w.r.t. varying numbers of training epochs on several hard and super hard maps. We observe a potential detrimental effect from an excessively large epoch number: when training with 15 epochs, MAPPO consistently learns a suboptimal policy, with particularly poor performance in the very difficult *MMM2* and *Corridor* maps. In comparison, MAPPO generally performs much better when using 5 or 10 epochs.

The performance of MAPPO is also impacted significantly by the number of mini-batches per training epoch. We

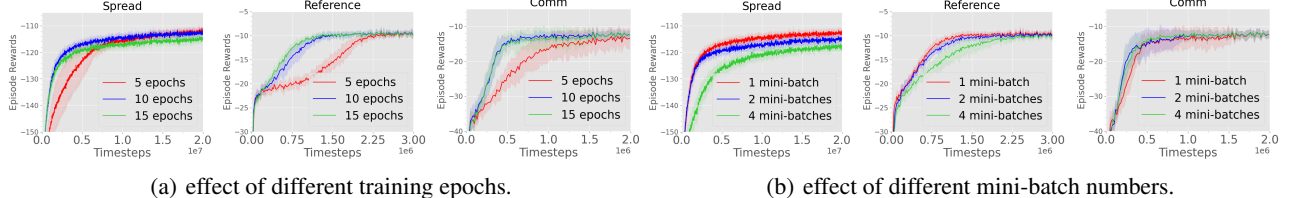


Figure 7. Ablation studies demonstrating the effect of epoch and mini-batch number on MAPPO’s performance in MPE.

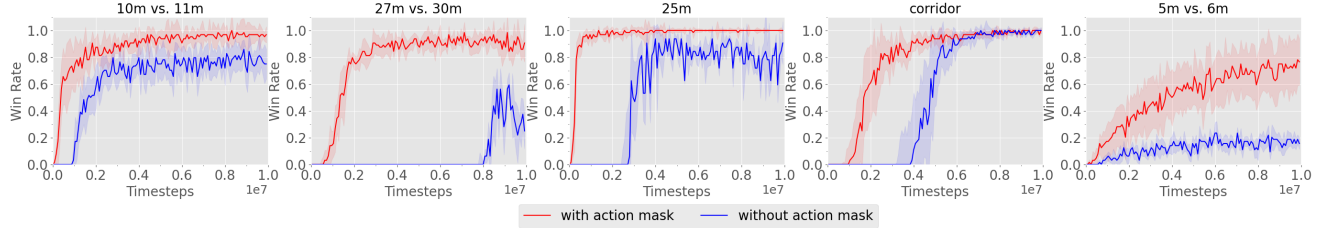


Figure 8. Ablation studies demonstrating the effect of action mask on MAPPO’s performance in SMAC.

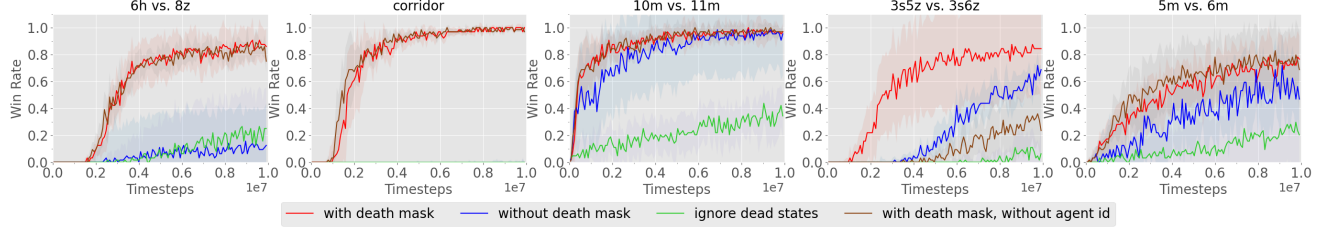


Figure 9. Ablation studies demonstrating the effect of death mask on MAPPO’s performance in SMAC.

consider three mini-batch values: 1, 2, and 4. A mini-batch of 4 indicates that we split the training data into 4 mini-batches to run gradient descent. The results in Fig. 6(b) indicate that using more mini-batches negatively affects the performance of MAPPO; when using 4 mini-batches, MAPPO fails to solve any of the selected maps while using 1 mini-batch produces the best performance on 22/23 maps. The only exception is the MMM2 map, in which using 2 mini-batches yields a small improvement.

We also evaluate different training epochs and mini-batches in the MPE tasks in Fig. 7. In *Reference* and *Comm*, the simplest MPE tasks, all chosen epoch and minibatch values result in the same final performance, and using 15 training epochs even leads to faster convergence. However, in the harder *Spread* task, we can observe a similar trend to SMAC: fewer epochs and no mini-batch splitting produces the highest rewards. Hence, we suggest to (1) use fewer training epochs as the multi-agent task becomes more challenging, particularly when agent numbers grow, and (2) not split data into mini-batches by default, and check small mini-batch values for potential performance improvements.

6.4. Action Masking

We evaluate the effect of using action masking in 5 selected SMAC maps in Fig. 8. We observe that using an action mask benefits MAPPO’s performance in general. In Corridor, the

use of the action mask improves training speed, and in the other maps which are shown, using an action mask sharply improves the final win rate. We thus recommend to always implement action masking in environments in which certain actions can be unavailable to agents.

6.5. Death Masking

We consider 4 death masking variants: (1) our suggested death masking, in which we replace the value state for a dead agent with a zero state containing the agent ID; (2) standard MAPPO implementation without death masking, i.e., still using the global state as value input; (3) completely ignoring the timesteps after an agent dies (note that we still need to accumulate rewards after the agent dies to correctly estimate episode returns); and (4) replacing the global state with a pure zero-state which does not include the agent ID. The evaluation results shown in Fig. 9 demonstrate that our agent-specific dead mask significantly outperforms variant (2) and variant (3), and consistently achieves overall strong performance. Including the agent id in the death mask, as is done in variant (1), is particularly important in maps with heterogeneous agents, as demonstrated by the superior performance of variant (1) compared to variant (4), which does not contain the agent id in the death-mask zero-state, in the 3s5z vs. 3s6z map. Therefore, we always suggest to use our death masking technique. Further justifications for the death mask can be found in Appendix B.

7. Conclusion

This work demonstrates that MAPPO, an on-policy policy gradient multi-agent reinforcement learning algorithm, achieves strong results comparable to the state-of-the-art on a variety of cooperative multi-agent challenges. Despite its on-policy nature, MAPPO is competitive to ubiquitous off-policy methods such as MADDPG, QMix, and RODE in terms of sample-efficiency and even exceeds the performance of these algorithms with respect to wall-clock time.

Additionally, in Section 4 and 6, we demonstrate 5 key algorithmic and implementation techniques that are important to MAPPO’s performance and support our findings with a variety of ablation studies which empirically demonstrate the effect of these techniques on MAPPO’s performance.

The strong results obtained by MAPPO suggest that properly configured MAPPO is a competitive baseline for MARL tasks. Building on these results, in future work, we aim to test the performance of MAPPO on a wider range of domains such as competitive games and multi-agent problems with continuous action spaces.

8. Acknowledgement

This work is supported by National Key R&D Program of China (2018YFB0105000). Eugene Vinitsky and Akash Velu were supported by the U.S. Department of Energy’s Office of Energy Efficiency and Renewable Energy (EERE) award number CID DE-EE0008872. The views expressed herein do not necessarily represent the views of the U.S. Department of Energy or the United States Government. The authors would like to thank Hengyuan Wu, Tonghan Wang, Shusheng Xu, Yuanfan Xu, Jiantao Qiu, Tianxiang Yang and Jianfei Cao for their support during this project. The authors would also like to thank Natasha Jaques, Michael Dennis, and Jakob Foerster for feedback on the work.

References

Andrychowicz, M., Raichuk, A., Stańczyk, P., Orsini, M., Girgin, S., Marinier, R., Hussenot, L., Geist, M., Pietquin, O., Michalski, M., Gelly, S., and Bachem, O. What matters for on-policy deep actor-critic methods? a large-scale study. In *International Conference on Learning Representations*, 2021.

Baker, B., Kanitscheider, I., Markov, T. M., Wu, Y., Powell, G., McGrew, B., and Mordatch, I. Emergent tool use from multi-agent autocurricula. In *8th International Conference on Learning Representations, ICLR 2020, Addis Ababa, Ethiopia, April 26-30, 2020*. OpenReview.net, 2020.

Bard, N., Foerster, J. N., Chandar, S., Burch, N., Lanctot, M., Song, H. F., Parisotto, E., Dumoulin, V., Moitra, S., Hughes, E., et al. The Hanabi challenge: A new frontier for AI research. *Artificial Intelligence*, 280:103216, 2020.

Berner, C., Brockman, G., Chan, B., Cheung, V., Debiak, P., Dennison, C., Farhi, D., Fischer, Q., Hashme, S., Hesse, C., Józefowicz, R., Gray, S., Olsson, C., Pachocki, J., Petrov, M., de Oliveira Pinto, H. P., Raiman, J., Salimans, T., Schlatter, J., Schneider, J., Sidor, S., Sutskever, I., Tang, J., Wolski, F., and Zhang, S. Dota 2 with large scale deep reinforcement learning. *CoRR*, abs/1912.06680, 2019.

Claus, C. and Boutilier, C. The dynamics of reinforcement learning in cooperative multiagent systems. *AAAI/IAAI*, 1998(746-752):2, 1998.

de Witt, C. S., Gupta, T., Makoviichuk, D., Makoviychuk, V., Torr, P. H. S., Sun, M., and Whiteson, S. Is independent learning all you need in the starcraft multi-agent challenge? *arXiv preprint arXiv:2011.09533*, 2020.

Dhariwal, P., Hesse, C., Klimov, O., Nichol, A., Plappert, M., Radford, A., Schulman, J., Sidor, S., Wu, Y., and Zhokhov, P. Openai baselines. <https://github.com/openai/baselines>, 2017.

Duan, Y., Chen, X., Houthooft, R., Schulman, J., and Abbeel, P. Benchmarking deep reinforcement learning for continuous control. In *International conference on machine learning*, pp. 1329–1338, 2016.

Engstrom, L., Ilyas, A., Santurkar, S., Tsipras, D., Janoos, F., Rudolph, L., and Madry, A. Implementation matters in deep rl: A case study on ppo and trpo. In *International Conference on Learning Representations*, 2020.

Espeholt, L., Soyer, H., Munos, R., Simonyan, K., Mnih, V., Ward, T., Doron, Y., Firoiu, V., Harley, T., Dunning, I., et al. Impala: Scalable distributed deep-rl with importance weighted actor-learner architectures. In *International Conference on Machine Learning*, pp. 1407–1416, 2018.

Foerster, J., Farquhar, G., Afouras, T., Nardelli, N., and Whiteson, S. Counterfactual multi-agent policy gradients. In *Proceedings of the Thirty-Second AAAI Conference on Artificial Intelligence*, 2018.

Haarnoja, T., Zhou, A., Abbeel, P., and Levine, S. Soft actor-critic: Off-policy maximum entropy deep reinforcement learning with a stochastic actor. *arXiv preprint arXiv:1801.01290*, 2018.

Hessel, M., Modayil, J., Van Hasselt, H., Schaul, T., Ostrovski, G., Dabney, W., Horgan, D., Piot, B., Azar, M., and Silver, D. Rainbow: Combining improvements in deep reinforcement learning. In *Proceedings of the AAAI Conference on Artificial Intelligence*, volume 32, 2018.

Hessel, M., Soyer, H., Espeholt, L., Czarnecki, W., Schmitt, S., and Hasselt, H. V. Multi-task deep reinforcement learning with popart. In *AAAI*, 2019.

Hsu, C. C.-Y., Mendler-Dünner, C., and Hardt, M. Revisiting design choices in proximal policy optimization. *arXiv preprint arXiv:2009.10897*, 2020.

Hu, H. and Foerster, J. N. Simplified action decoder for deep multi-agent reinforcement learning. In *International Conference on Learning Representations*, 2020.

Hu, H., Lerer, A., Brown, N., and Foerster, J. N. Learned belief search: Efficiently improving policies in partially observable settings, 2021. URL https://openreview.net/forum?id=xP37gkVKa_0.

Ilyas, A., Engstrom, L., Santurkar, S., Tsipras, D., Janoos, F., Rudolph, L., and Madry, A. A closer look at deep policy gradients. In *International Conference on Learning Representations*, 2020.

Kleinberg, B., Li, Y., and Yuan, Y. An alternative view: When does sgd escape local minima? In *International Conference on Machine Learning*, pp. 2698–2707. PMLR, 2018.

Littman, M. L. Markov games as a framework for multi-agent reinforcement learning. In *Machine learning proceedings 1994*, pp. 157–163. Elsevier, 1994.

Liu, Z., Li, X., Kang, B., and Darrell, T. Regularization matters in policy optimization—an empirical study on continuous control. *arXiv preprint arXiv:1910.09191*, 2019.

Lowe, R., Wu, Y., Tamar, A., Harb, J., Abbeel, P., and Mordatch, I. Multi-agent actor-critic for mixed cooperative-competitive environments. *Neural Information Processing Systems (NIPS)*, 2017.

Mahmood, A. R., Korenkevych, D., Vasan, G., Ma, W., and Bergstra, J. Benchmarking reinforcement learning algorithms on real-world robots. In *Conference on robot learning*, pp. 561–591. PMLR, 2018.

Mordatch, I. and Abbeel, P. Emergence of grounded compositional language in multi-agent populations. *arXiv preprint arXiv:1703.04908*, 2017.

Oliehoek, F. A., Amato, C., et al. *A concise introduction to decentralized POMDPs*, volume 1. Springer, 2016.

Panait, L. and Luke, S. Cooperative multi-agent learning: The state of the art. *Autonomous agents and multi-agent systems*, 11(3):387–434, 2005.

Papoudakis, G., Christianos, F., Schäfer, L., and Albrecht, S. V. Comparative evaluation of multi-agent deep reinforcement learning algorithms. *arXiv preprint arXiv:2006.07869*, 2020.

Rashid, T., Samvelyan, M., Schroeder, C., Farquhar, G., Foerster, J., and Whiteson, S. QMIX: Monotonic value function factorisation for deep multi-agent reinforcement learning. volume 80 of *Proceedings of Machine Learning Research*, pp. 4295–4304. PMLR, 10–15 Jul 2018.

Rashid, T., Torr, P. H., Farquhar, G., Hung, C.-M., Rudner, T. G., Nardelli, N., Whiteson, S., de Witt, C. S., Foerster, J., and Samvelyan, M. The Starcraft multi-agent challenge. volume 4, pp. 2186–2188. International Foundation for Autonomous Agents and Multiagent Systems, 2019.

Schulman, J., Moritz, P., Levine, S., Jordan, M., and Abbeel, P. High-dimensional continuous control using generalized advantage estimation. In *Proceedings of the International Conference on Learning Representations (ICLR)*, 2016.

Schulman, J., Wolski, F., Dhariwal, P., Radford, A., and Klimov, O. Proximal policy optimization algorithms. *CoRR*, abs/1707.06347, 2017.

Son, K., Kim, D., Kang, W. J., Hostallero, D. E., and Yi, Y. Qtran: Learning to factorize with transformation for cooperative multi-agent reinforcement learning. In *International Conference on Machine Learning*, pp. 5887–5896. PMLR, 2019.

Stooke, A. and Abbeel, P. rlpyt: A research code base for deep reinforcement learning in pytorch. *arXiv preprint arXiv:1909.01500*, 2019.

Sunehag, P., Lever, G., Gruslys, A., Czarnecki, W. M., Zambaldi, V., Jaderberg, M., Lanctot, M., Sonnerat, N., Leibo, J. Z., Tuyls, K., et al. Value-decomposition networks for cooperative multi-agent learning based on team reward. In *Proceedings of the 17th International Conference on Autonomous Agents and MultiAgent Systems*, pp. 2085–2087, 2018.

Tucker, G., Bhupatiraju, S., Gu, S., Turner, R., Ghahramani, Z., and Levine, S. The mirage of action-dependent baselines in reinforcement learning. In *International conference on machine learning*, pp. 5015–5024. PMLR, 2018.

Vinyals, O., Babuschkin, I., Czarnecki, M. W., Mathieu, M., Dudzik, A., Chung, J., Choi, H. D., Powell, R., Ewalds, T., Georgiev, P., Oh, J., Horgan, D., Kroiss, M., Danihelka, I., Huang, A., Sifre, L., Cai, T., Agapiou, P. J., Jaderberg, M., Vezhnevets, S. A., Leblond, R., Pohlen, T., Dalibard, V., Budden, D., Sulsky, Y., Molloy, J., Paine, L. T., Gulcehre, C., Wang, Z., Pfaff, T., Wu, Y., Ring, R., Yogatama, D., Wünsch, D., McKinney, K., Smith, O., Schaul, T., Lillicrap, T., Kavukcuoglu, K., Hassabis, D., Apps, C., and Silver, D. Grandmaster level in starcraft ii using multi-agent reinforcement learning. *Nature*, pp. 1–5, 2019.

Wang, T., Gupta, T., Mahajan, A., Peng, B., Whiteson, S.,
and Zhang, C. RODE: Learning roles to decompose multi-
agent tasks. In *International Conference on Learning
Representations*, 2021.

A. MAPPO Details

Algorithm 1 Recurrent-MAPPO

```

Initialize  $\theta$ , the parameters for policy  $\pi$  and  $\phi$ , the parameters for critic  $V$ , using Orthogonal initialization (Hu et al., 2020)
Set learning rate  $\alpha$ 
while  $step \leq step_{max}$  do
    set data buffer  $D = \{\}$ 
    for  $i = 1$  to  $batch\_size$  do
         $\tau = []$  empty list
        initialize  $h_{0,\pi}^{(1)}, \dots, h_{0,\pi}^{(n)}$  actor RNN states
        initialize  $h_{0,V}^{(1)}, \dots, h_{0,V}^{(n)}$  critic RNN states
        for  $t = 1$  to  $T$  do
            for all agents  $a$  do
                 $p_t^{(a)}, h_{t,\pi}^{(a)} = \pi(o_t^{(a)}, h_{t-1,\pi}^{(a)}; \theta)$ 
                 $u_t^{(a)} \sim p_t^{(a)}$ 
                 $v_t^{(a)}, h_{t,V}^{(a)} = V(s_t^{(a)}, h_{t-1,V}^{(a)}; \phi)$ 
            end for
            Execute actions  $u_t$ , observe  $r_t, s_{t+1}, o_{t+1}$ 
             $\tau += [s_t, o_t, h_{t,\pi}, h_{t,V}, u_t, r_t, s_{t+1}, o_{t+1}]$ 
        end for
        Compute advantage estimate  $\hat{A}$  via GAE on  $\tau$ , using PopArt
        Compute reward-to-go  $\hat{R}$  on  $\tau$  and normalize with PopArt
        Split trajectory  $\tau$  into chunks of length  $L$ 
        for  $l = 0, 1, \dots, T//L$  do
             $D = D \cup (\tau[l : l + T, \hat{A}[l : l + L], \hat{R}[l : l + L]])$ 
        end for
    end for
    for mini-batch  $k = 1, \dots, K$  do
         $b \leftarrow$  random mini-batch from  $D$  with all agent data
        for each data chunk  $c$  in the mini-batch  $b$  do
            update RNN hidden states for  $\pi$  and  $V$  from first hidden state in data chunk
        end for
    end for
    Adam update  $\theta$  on  $L(\theta)$  with data  $b$ 
    Adam update  $\phi$  on  $L(\phi)$  with data  $b$ 
end while

```

MAPPO trains two separate neural networks: an actor network with parameters θ , and a value function network (referred to as a critic) with parameters ϕ . These networks can be shared amongst all agents if the agents are homogeneous, but each agent can also have its own pair of actor and critic networks. We assume here that all agents share critic and actor networks, for notational convenience. Specifically, the critic network, denoted as V_ϕ , performs the following mapping: $S \rightarrow \mathbb{R}$. The global state can be agent-specific or agent-agnostic.

The actor network, denoted as π_θ , maps agent observations $o_t^{(a)}$ to a categorical distribution over actions in discrete action spaces, or to the mean and standard deviation vectors of a Multivariate Gaussian Distribution, from which an action is sampled, in continuous action spaces.

The actor network is trained to maximize $L(\theta) = [\frac{1}{Bn} \sum_{i=1}^B \sum_{k=1}^n \min(r_{\theta,i}^{(k)} A_i^{(k)}, \text{clip}(r_{\theta,i}^{(k)}, 1 - \epsilon, 1 + \epsilon) A_i^{(k)})] + \sigma \frac{1}{Bn} \sum_{i=1}^B \sum_{k=1}^n S[\pi_\theta(o_i^{(k)})]$, where $r_{\theta,i}^{(k)} = \frac{\pi_\theta(a_i^{(k)} | o_i^{(k)})}{\pi_{\theta_{old}}(a_i^{(k)} | o_i^{(k)})}$. $A_i^{(k)}$ is computed using the GAE method, S is the policy entropy, and σ is the entropy coefficient hyperparameter.

The critic network is trained to minimize the loss function $L(\phi) = \frac{1}{Bn} \sum_{i=1}^B \sum_{k=1}^n (\max[(V_\phi(s_i^{(k)}) - \hat{R}_i)^2, (\text{clip}(V_\phi(s_i^{(k)}), V_{\phi_{old}}(s_i^{(k)}), \epsilon, V_{\phi_{old}}(s_i^{(k)}) + \epsilon) - \hat{R}_i)^2]]$, where \hat{R}_i is the discounted reward-to-go.

In the loss functions above, B refers to the batch size and n refers to the number of agents.

If the critic and actor networks are RNNs, then the loss functions additionally sum over time, and the networks are trained via Backpropagation Through Time (BPTT). Pseudocode for recurrent-MAPPO is shown in Alg. 1.

B. Justification of Death Masking

Let $\mathbf{0}_a$ be a zero vector with agent a 's agent ID appended to the end. The use of agent ID leads to an agent-specific value function depending on an agent's type or role. It has been empirically justified in Sec. 6.5 that such an agent-specific feature is particularly helpful when the environment contains heterogeneous agents.

We now provide some intuition as to why using $\mathbf{0}_a$ as the critic input when agents are dead appears to be a better alternative to using the usual agent-specific global state as the input to the value function. Note that our global state to the value network has agent-specific information, such as available actions and relative distances to other agents. When an agent dies, these agent-specific features become zero, while the remaining agent-agnostic features remain nonzero - this leads to a drastic distribution shift in the critic input compared to states in which the agent is alive. In most SMAC maps, an agent is dead in only a small fraction of the timesteps in a batch (about 20%); due to their relative infrequency in the training data the states in which an agent is dead will likely have large value prediction error. Moreover, it is also possible that training on these out of distribution inputs harms the feature representation of the value network.

Although replacing the states at which an agent is dead with a fixed vector $\mathbf{0}_a$ also results in a distribution shift,

the replacement results in there being only 1 vector which captures the state at which an agent is dead - thus, the critic is more likely to be able to fit the average post-death reward for agent a to the input 0_a . Our ablation on the value function fitting error provide some weight to this hypothesis.

Another possible mechanism of handling agent deaths is to completely skip value learning in states in which an agent is dead, by essentially terminating an agent’s episode when it dies. Suppose the game episode is T and the agent dies at timestep d . If we are not learning on dead state then, in order to correctly accumulate the episode return, we need to replace the reward r_d at timestep d by the total return R_d at time d , i.e., $r_d \leftarrow R_d = \sum_{t=d}^T \gamma^{t-d} r_t$. We would then need to compute the GAE only on those states in which the agent is alive. While this approach is theoretically correct (we are simply treating the state where the agent died as a terminal state and assigning the accumulated discounted reward as a terminal reward), it can have negative ramifications in the policy learning process, as outlined below.

The GAE is an exponentially weighted average of k -step returns intended to trade off between bias and variance. Large k values result in a low bias, but high variance return estimate, whereas small k values result in a high bias, low variance return estimate. However, since the entire post death return R_d replaces the single timestep reward r_d at timestep d , computing the 1-step return estimate at timestep d essentially becomes a $(T - d)$ -step estimate, eliminating potential benefits of value function truncation of the trajectory and potentially leading to higher variance. This potentially dampens the benefit that could come from using the GAE at the timesteps in which an agent is dead.

We analyze the impact of the death masking by comparing different ways of handling dead agents, including: (1) our death masking, (2) using global states without death masking and (3) ignoring dead states in value learning and in the GAE computation. We first examine the median win rate with these different options in Fig. 18 and 19. It is evident that our method of death masking, which uses 0_a as the input to the critic when an agent is dead, results in superior performance compared to other options.

Additionally, Fig. 20 demonstrates that using the death mask results in a lower values loss in the vast majority of SMAC maps, demonstrating that the accuracy of the value predictions improve when using the death mask. While the arguments here are intuitive the clear experimental benefits suggest that theoretically characterizing the effect of this method would be valuable.

C. Testing domains

Multi-agent Particle-World Environment (MPE) was introduced in (Lowe et al., 2017). MPE consist of various

multi-agent games in a 2D world with small particles navigating within a square box. We consider the 3 fully cooperative tasks from the original set shown in Fig. 10(a): *Spread*, *Comm*, and *Reference*. Note that since the two agents in *speaker-listener* have different observation and action spaces, this is the only setting in this paper where we do not share parameters but train separate policies for each agent.

StarCraftII Micromanagement Challenge (SMAC) tasks were introduced in (Rashid et al., 2019). In these tasks, decentralized agents must cooperate to defeat adversarial bots in various scenarios with a wide range of agent numbers (from 2 to 27). We use a global game state to train our centralized critics or Q-functions. Fig. 10(c) and 10(d) show two example StarCraftII environments.

As described in Sec. 4.2, we utilize an agent-specific global state as input to the global state. This agent-specific global state augments the original global state provided by the SMAC environment by adding relevant agent-specific features.

Specifically, the original global state of SMAC contains information about all agents and enemies - this includes information such as the distance from each agent/enemy to the map center, the health of each agent/enemy, the shield status of each agent/enemy, and the weapon cooldown state of each agent. However, when compared to the local observation of each agent, the global state does not contain agent-specific information including agent id, agent movement options, agent attack options, relative distance to allies/enemies. Note that the local observation contains information only about allies/enemies within a sight radius of the agent. We form the agent-specific global state by adding these features to the original global state.

Hanabi is a turn-based card game, introduced as a MARL challenge in (Bard et al., 2020), where each agent observes other players’ cards except their own cards. A visualization of the game is shown in Fig. 3. The goal of the game is to send information tokens to others and cooperatively take actions to stack as many cards as possible in ascending order to collect points.

The turn-based nature of Hanabi presents a challenge when computing the reward for an agent during it’s turn. We utilize the forward accumulated reward as one turn reward R_i ; specifically, if there are 4 players and players 0, 1, 2, and 3 execute their respective actions at timesteps k , $k+1$, $k+2$, $k+3$ respectively, resulting in rewards of $r_k^{(0)}, r_{k+1}^{(1)}, r_{k+2}^{(2)}, r_{k+3}^{(3)}$, then the reward assigned to player 0 will be $R_0 = r_k^{(0)} + r_{k+1}^{(1)} + r_{k+2}^{(2)} + r_{k+3}^{(3)}$ and similarly, the reward assigned to player 1 will be $R_1 = r_{k+1}^{(1)} + r_{k+2}^{(2)} + r_{k+3}^{(3)} + r_{k+4}^{(0)}$. Here, r_t^i denotes the reward received at timestep t when agent i executes a move.

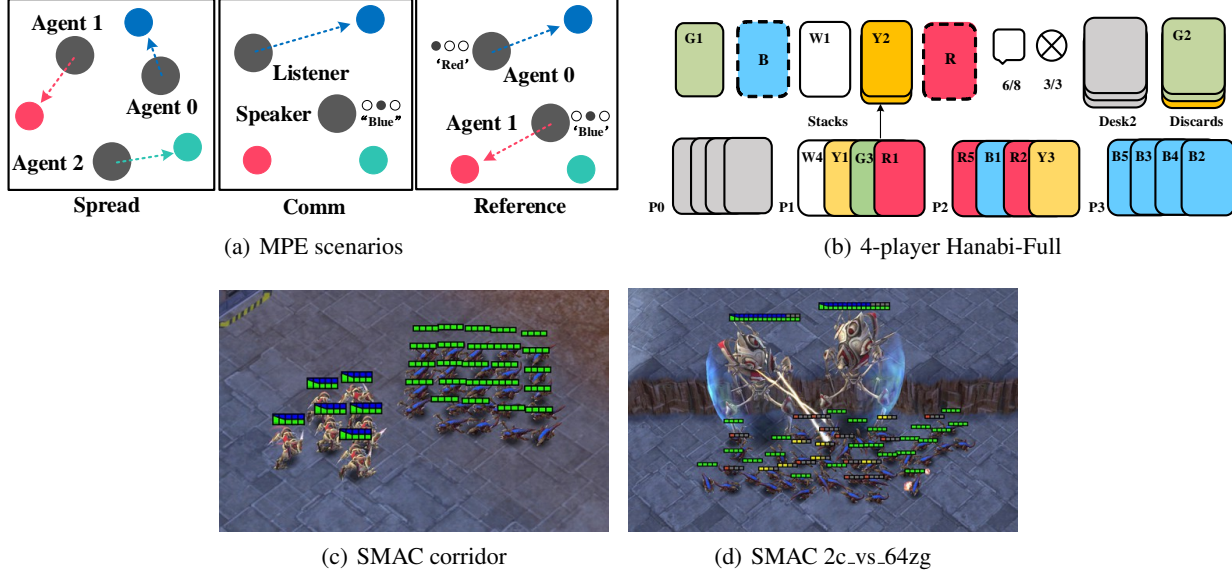


Figure 10. Task visualizations. (a) The MPE domain. *Spread* (left): agents need to cover all the landmarks and do not have a color preference for the landmark they navigate to; *Comm* (middle): the listener needs to navigate to a specific landmarks following the instruction from the speaker; *Reference* (right): both agents only know the other’s goal landmark and needs to communicate to ensure both agents move to the desired target. (b) The Hanabi domain: 4-player *Hanabi-Full* - figure obtained from (Bard et al., 2020). (c) The *corridor* map in the SMAC domain. (d) The *2c vs. 64zg* map in the SMAC domain.

D. Training details

D.1. Implementation

All algorithms utilize parameter sharing - i.e., all agents share the same networks - in all environments except for the *Comm* scenario in the MPE. Furthermore, we tune the architecture and hyperparameters of MADDPG and QMix, and thus use different hyperparameters than the original implementations. However, we ensure that the performance of the algorithms in the baselines matches or exceeds the results reported in their original papers.

For each algorithm, certain hyperparameters are kept constant across all environments; these are listed in Tables 3 and 4 for MAPPO, QMix, and MADDPG, respectively. These values are obtained either from the PPO baselines implementation in the case of MAPPO, or from the original implementations for QMix and MADDPG. Note that since we use parameter sharing and combine all agents’ data, the actual batch-sizes will be larger with more agents.

In these tables, “recurrent data chunk length” refers to the length of chunks that a trajectory is split into before being used for training via BPTT (only applicable for RNN policies). “Max clipped value loss” refers to the value-clipping term in the value loss. “Gamma” refers to the discount factor, and “huber delta” specifies the delta parameter in the Huber loss function. “Epsilon” describes the starting and ending value of ϵ for ϵ -greedy exploration, and “epsilon anneal time” refers to the number of environment steps over which ϵ will be annealed from the starting to the ending value, in a linear manner. “Use feature normalization” refers to whether the

feature normalization is applied to the network input.

D.2. Hyperparameters

Tables 3-11 describe the common hyperparameters, hyperparameter grid search values, and chosen hyperparameters for MAPPO, QMix, and MADDPG in all testing domains. Tables 5, 6, and 7 describe common hyperparameters for different algorithms in each domain. Tables 8, 9, and 10 describe the hyperparameter grid search procedure for the MAPPO, QMix, and MADDPG algorithms, respectively. Lastly, Tables 11, 12, and 13 describe the final chosen hyperparameters among fine-tuned parameters for different algorithms in MPE, SMAC, and Hanabi, respectively.

For MAPPO, “Batch Size” refers to the number of environment steps collected before updating the policy via gradient descent. Since agents do not share a policy only in the MPE speaker-listener, the batch size does not depend on the number of agents in the speaker-listener environment. “Minibatch” refers to the number of mini-batches a batch of data is split into, “gain” refers to the weight initialization gain of the last network layer for the actor network. “Entropy coef” is the entropy coefficient σ in the policy loss. “Tau” corresponds to the rate of the polyak average technique used to update the target networks, and if the target networks are not updated in a “soft” manner, the “hard interval” hyperparameter specifies the number of gradient updates which must elapse before the target network parameters are updated to equal the live network parameters.

MLP network architectures are as follows: all MLP net-

works use “num fc” linear layers, whose dimensions are specified by the “fc layer dim” hyperparameter. When using MLP networks, “stacked frames” refers to the number of previous observations which are concatenated to form the network input: for instance, if “stacked frames” equals 1, then only the current observation is used as input, and if “stacked frames” is 2, then the current and previous observations are concatenated to form the input. For RNN networks, the network architecture is “num fc” fully connected linear layers of dimension “fc layer dim”, followed by “num GRU layers” GRU layers, finally followed by “num fc after” linear layers.

E. Additional Results

E.1. Additional SMAC Results

As MAPPO does not converge within 10M environment steps in the 3s5z vs. 3s6z map, Fig. 11 shows the performance of MAPPO in 3s5z vs. 3s6z when run until convergence. Fig. 12 presents the evaluation win rate of all 23 maps in SMAC domain. *MAPPO-original* curves refer to MAPPO results obtained using the original global state as opposed to the agent-specific global state (which is used for the *MAPPO* curves). For each algorithm, each map is run for at least 6 seeds. For more difficult maps, we run 10-20 seeds. Fig. 13 shows the evaluation win rate of MAPPO compared to RODE and QMix, in the maps in which RODE’s results are available.

F. Ablation Studies

We present the learning curves for all ablation studies performed. Fig. 14 demonstrates the impact of PopArt value normalization on MAPPO’s performance. Fig. 15 shows the effect of global state information on MAPPO’s performance in SMAC. Fig. 16 studies the influence of training epochs on MAPPO’s performance. Fig. 17 demonstrates the effect of the action mask on MAPPO’s performance. Fig. 18 illustrates the influence of the death mask on MAPPO’s performance. Similarly, Fig. 19 compares the performance of MAPPO when ignoring states in which an agent is dead when computing GAE to using the death mask when computing the GAE. Fig. 20 illustrates the effect of death mask on MAPPO’s value loss in the SMAC domain. Lastly, Fig. 21 shows the influence of including the agent-id in the agent-specific global state.

| common hyperparameters | value |
|-----------------------------|---|
| recurrent data chunk length | 10 |
| max clipped value loss | 0.2 |
| gradient clip norm | 10.0 |
| gae lambda | 0.95 |
| gamma | 0.99 |
| value loss | huber loss |
| huber delta | 10.0 |
| batch size | num envs \times buffer length \times num agents |
| mini batch size | batch size / mini-batch |
| optimizer | Adam |
| optimizer epsilon | 1e-5 |
| weight decay | 0 |
| network initialization | Orthogonal |
| use reward normalization | True |
| use feature normalization | True |

Table 3. Common hyperparameters used in MAPPO across all domains.

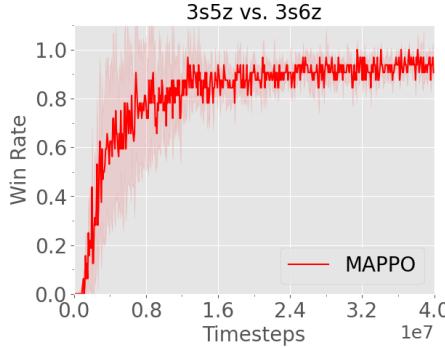


Figure 11. Median win rate of 3s5z vs. 3s6z map after 40M environment steps.

| common hyperparameters | value |
|---------------------------|------------------------|
| gradient clip norm | 10.0 |
| random episodes | 5 |
| epsilon | 1.0 \rightarrow 0.05 |
| epsilon anneal time | 50000 timesteps |
| train interval | 1 episode |
| gamma | 0.99 |
| critic loss | mse loss |
| buffer size | 5000 episodes |
| batch size | 32 episodes |
| optimizer | Adam |
| optimizer eps | 1e-5 |
| weight decay | 0 |
| network initialization | Orthogonal |
| use reward normalization | True |
| use feature normalization | True |

Table 4. Common hyperparameters used in QMix and MADDPG across all domains.

| hyperparameters | value |
|----------------------|------------|
| num envs | MAPPO: 128 |
| buffer length | MAPPO: 25 |
| num GRU layers | 1 |
| RNN hidden state dim | 64 |
| fc layer dim | 64 |
| num fc | 2 |
| num fc after | 1 |

Table 5. Common hyperparameters used in the MPE domain for MAPPO, MADDPG, and QMix.

| hyperparameters | value |
|----------------------|------------|
| num envs | MAPPO:8 |
| buffer length | MAPPO: 400 |
| num GRU layers | 1 |
| RNN hidden state dim | 64 |
| fc layer dim | 64 |
| num fc | 2 |
| num fc after | 1 |

Table 6. Common hyperparameters used in the SMAC domain for MAPPO and QMix.

| hyperparameters | value |
|-----------------|-------|
| num envs | 1000 |
| buffer length | 100 |
| fc layer dim | 512 |
| num fc | 2 |

Table 7. Common hyperparameters used in the Hanabi domain for MAPPO.

| Domains | lr | epoch | mini-batch | activation | gain | entropy coef | network |
|---------|-----------------------|--------------|------------|-------------|----------|---------------|-----------|
| MPE | [1e-4,5e-4,7e-4,1e-3] | [5,10,15,20] | [1,2,4] | [ReLU,Tanh] | [0.01,1] | / | [mlp,rnn] |
| SMAC | [1e-4,5e-4,7e-4,1e-3] | [5,10,15] | [1,2,4] | [ReLU,Tanh] | [0.01,1] | / | [mlp,rnn] |
| Hanabi | [1e-4,5e-4,7e-4,1e-3] | [5,10,15] | [1,2,4] | [ReLU,Tanh] | [0.01,1] | [0.01, 0.015] | [mlp,rnn] |

Table 8. Sweeping procedure of MAPPO cross all domains.

| Domains | lr | tau | hard interval | activation | gain |
|---------|-----------------------|--------------------|---------------|-------------|----------|
| MPE | [1e-4,5e-4,7e-4,1e-3] | [0.001,0.005,0.01] | [100,200,500] | [ReLU,Tanh] | [0.01,1] |
| SMAC | [1e-4,5e-4,7e-4,1e-3] | [0.001,0.005,0.01] | [100,200,500] | [ReLU,Tanh] | [0.01,1] |

Table 9. Sweeping procedure of QMix in the MPE and SMAC domains.

| Domains | lr | tau | activation | gain | network |
|---------|-----------------------|--------------------|-------------|----------|-----------|
| MPE | [1e-4,5e-4,7e-4,1e-3] | [0.001,0.005,0.01] | [ReLU,Tanh] | [0.01,1] | [mlp,rnn] |

Table 10. Sweeping procedure of MADDPG in the MPE domain.

| Scenarios | lr | gain | network | MAPPO | | | MADDPG | | | QMIX | |
|-----------|------|------|---------|-------|------------|------------|--------|------------|-------|---------------|------------|
| | | | | epoch | mini-batch | activation | tau | activation | tau | hard interval | activation |
| Spread | 7e-4 | 0.01 | rnn | 10 | 1 | Tanh | 0.005 | ReLU | / | 100 | ReLU |
| Reference | 7e-4 | 0.01 | rnn | 15 | 1 | ReLU | 0.005 | ReLU | 0.005 | / | ReLU |
| Comm | 7e-4 | 0.01 | rnn | 15 | 1 | Tanh | 0.005 | ReLU | 0.005 | / | ReLU |

Table 11. Adopted hyperparameters used for MAPPO, MADDPG and QMix in the MPE domain.

| Maps | lr | activation | MAPPO | | | | | QMIX | |
|------------------|------|------------|-------|------------|------|---------|----------------|---------------|------|
| | | | epoch | mini-batch | gain | network | stacked frames | hard interval | gain |
| 2m vs. 1z | 5e-4 | ReLU | 15 | 1 | 0.01 | rnn | 1 | 200 | 0.01 |
| 3m | 5e-4 | ReLU | 15 | 1 | 0.01 | rnn | 1 | 200 | 0.01 |
| 2s vs. 1sc | 5e-4 | ReLU | 15 | 1 | 0.01 | rnn | 1 | 200 | 0.01 |
| 3s vs. 3z | 5e-4 | ReLU | 15 | 1 | 0.01 | rnn | 1 | 200 | 0.01 |
| 3s vs. 4z | 5e-4 | ReLU | 15 | 1 | 0.01 | mlp | 4 | 200 | 0.01 |
| 3s vs. 5z | 5e-4 | ReLU | 15 | 1 | 0.01 | mlp | 4 | 200 | 0.01 |
| 2c vs. 64zg | 5e-4 | ReLU | 5 | 1 | 0.01 | rnn | 1 | 200 | 0.01 |
| so many baneling | 5e-4 | ReLU | 15 | 1 | 0.01 | rnn | 1 | 200 | 0.01 |
| 8m | 5e-4 | ReLU | 15 | 1 | 0.01 | rnn | 1 | 200 | 0.01 |
| MMM | 5e-4 | ReLU | 15 | 1 | 0.01 | rnn | 1 | 200 | 0.01 |
| 1c3s5z | 5e-4 | ReLU | 15 | 1 | 0.01 | rnn | 1 | 200 | 0.01 |
| 8m vs. 9m | 5e-4 | ReLU | 15 | 1 | 0.01 | rnn | 1 | 200 | 0.01 |
| bane vs. bane | 5e-4 | ReLU | 15 | 1 | 0.01 | rnn | 1 | 200 | 0.01 |
| 25m | 5e-4 | ReLU | 10 | 1 | 0.01 | rnn | 1 | 200 | 0.01 |
| 5m vs. 6m | 5e-4 | ReLU | 10 | 1 | 0.01 | rnn | 1 | 200 | 0.01 |
| 3s5z | 5e-4 | ReLU | 5 | 1 | 0.01 | rnn | 1 | 200 | 0.01 |
| MMM2 | 5e-4 | ReLU | 5 | 2 | 1 | rnn | 1 | 200 | 0.01 |
| 10m vs. 11m | 5e-4 | ReLU | 10 | 1 | 0.01 | rnn | 1 | 200 | 0.01 |
| 3s5z vs. 3s6z | 5e-4 | ReLU | 5 | 1 | 0.01 | rnn | 1 | 200 | 1 |
| 27m vs. 30m | 5e-4 | ReLU | 5 | 1 | 0.01 | rnn | 1 | 200 | 1 |
| 6h vs. 8z | 5e-4 | ReLU | 5 | 1 | 0.01 | mlp | 1 | 200 | 1 |
| corridor | 5e-4 | ReLU | 5 | 1 | 0.01 | mlp | 1 | 200 | 1 |

Table 12. Adopted hyperparameters used for MAPPO and QMix in the SMAC domain.

| Tasks | MAPPO | | | | | | |
|----------|---------------------------|-------|------------|------------|------|--------------|---------|
| | lr | epoch | mini-batch | activation | gain | entropy coef | network |
| 2-player | actor:7e-4 critic:1e-3 | 15 | 1 | ReLU | 0.01 | 0.015 | mlp |

Table 13. Adopted hyperparameters used for MAPPO in the Hanabi domain.

The Surprising Effectiveness of MAPPO in Cooperative, Multi-Agent Games

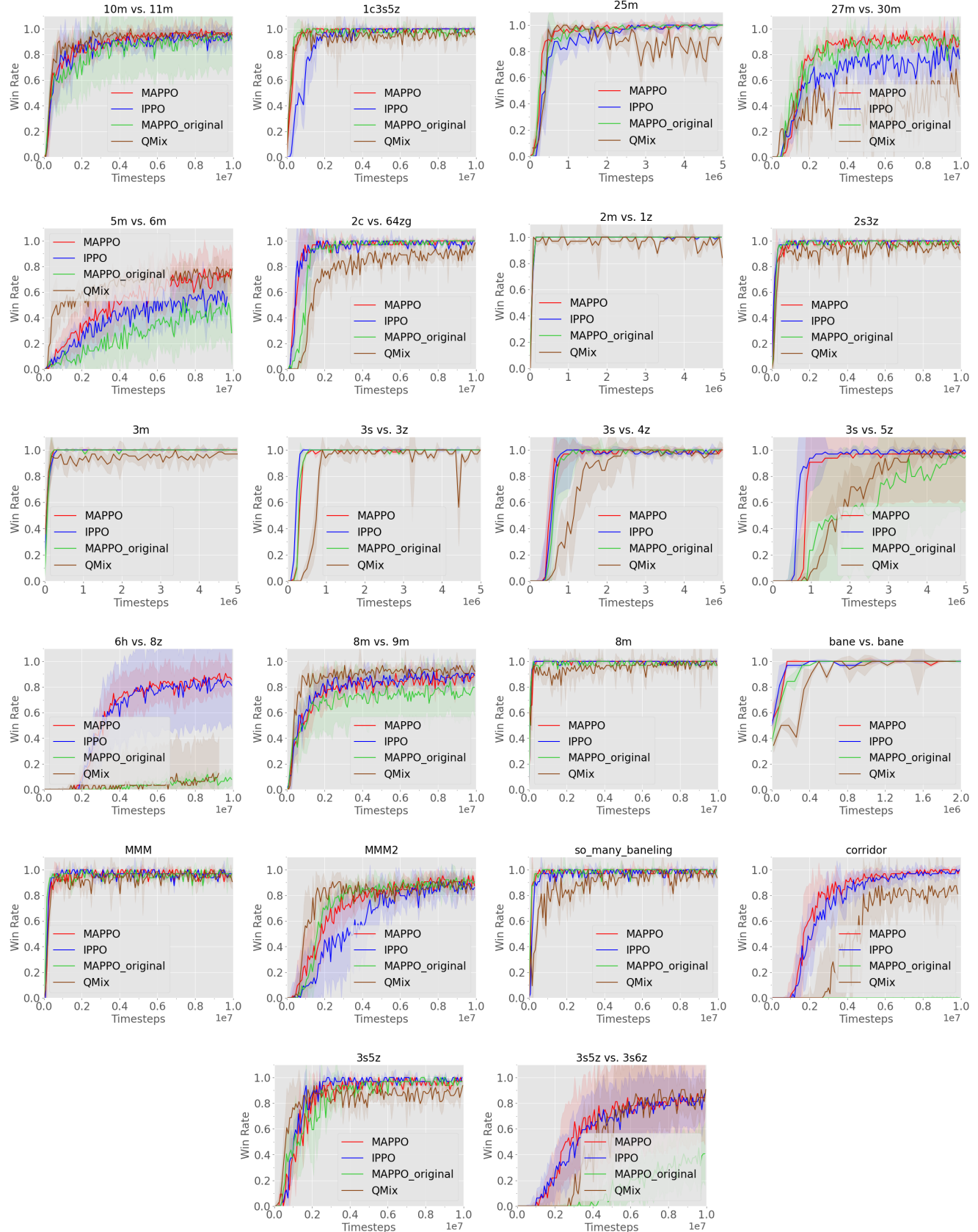


Figure 12. Median evaluation win rate of 23 maps in the SMAC domain.

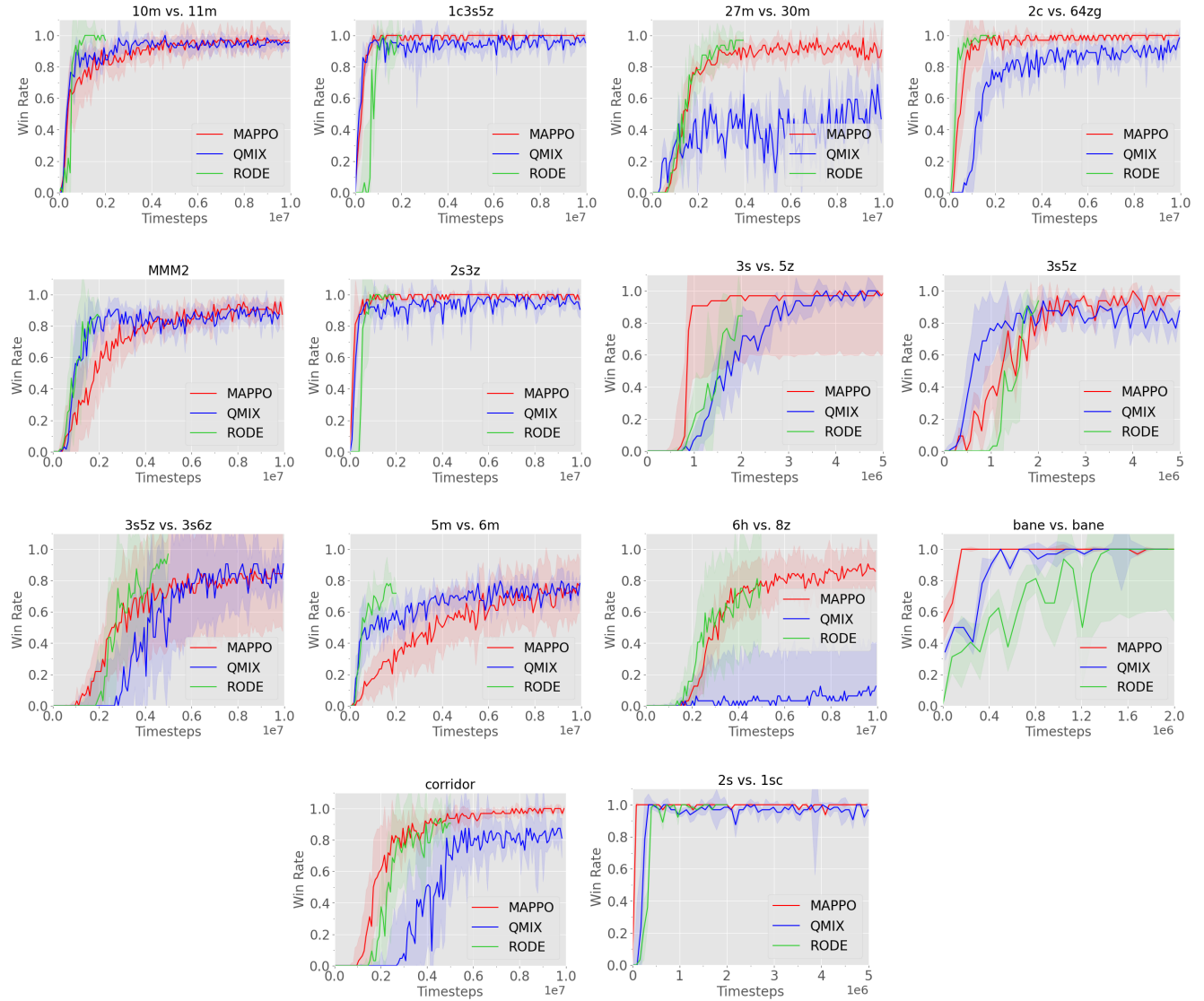


Figure 13. Median evaluation win rate of MAPPO, RODE, QMix in the SMAC domain.

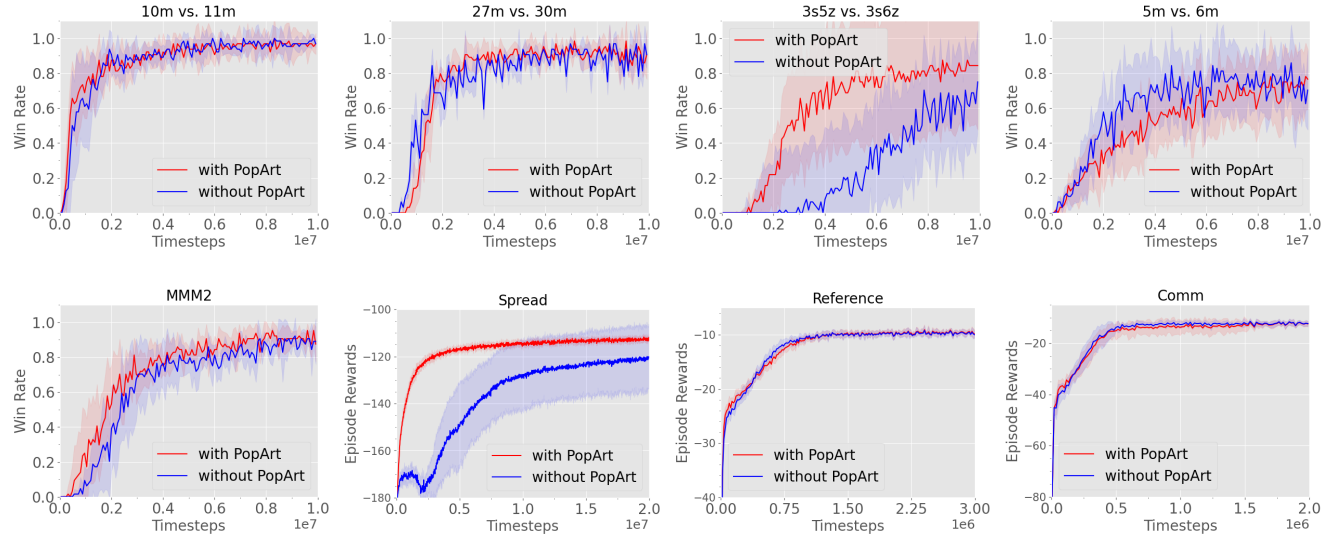


Figure 14. Ablation studies demonstrating the effect of PopArt on MAPPO’s performance in the SMAC and MPE domains.

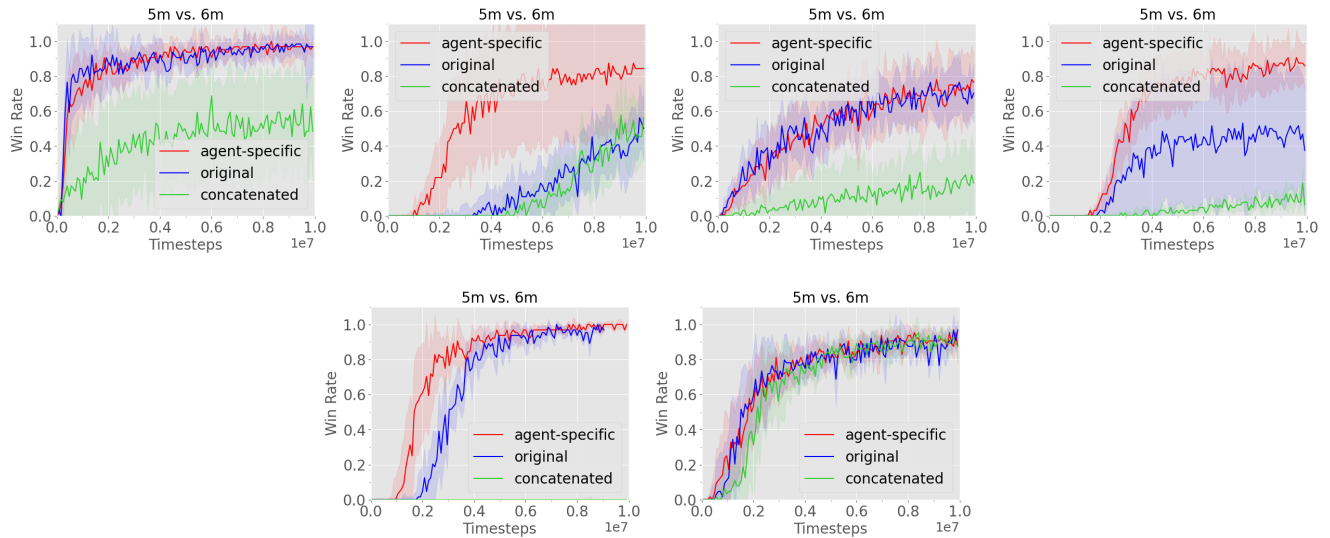


Figure 15. Ablation studies demonstrating the effect of different global state on MAPPO’s performance in the SMAC domain.

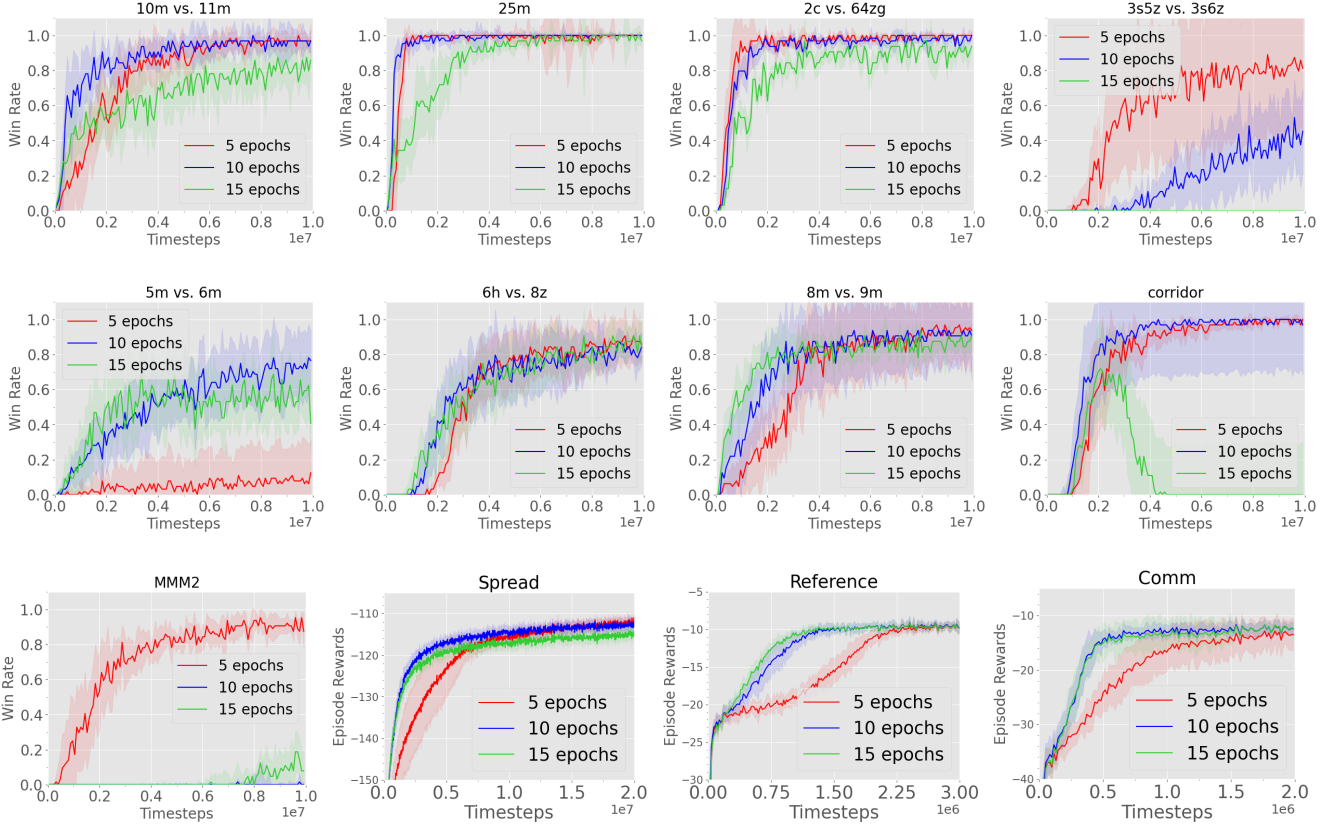


Figure 16. Ablation studies demonstrating the effect of training epochs on MAPPO’s performance in the SMAC and MPE domains.

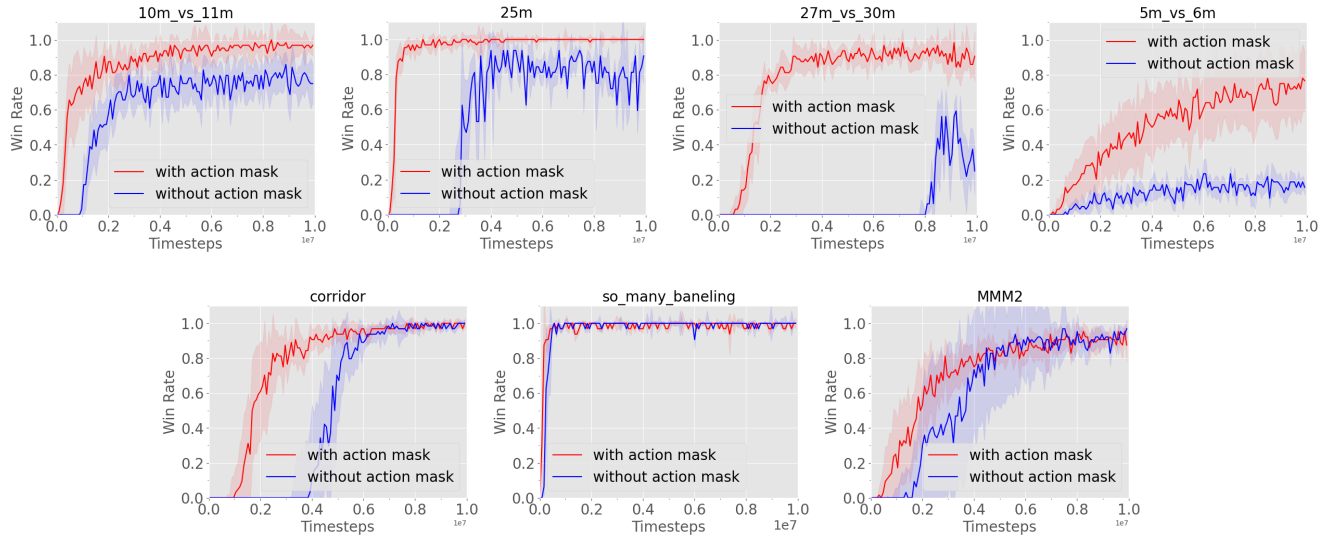


Figure 17. Ablation studies demonstrating the effect of action mask on MAPPO’s performance in the SMAC domain.

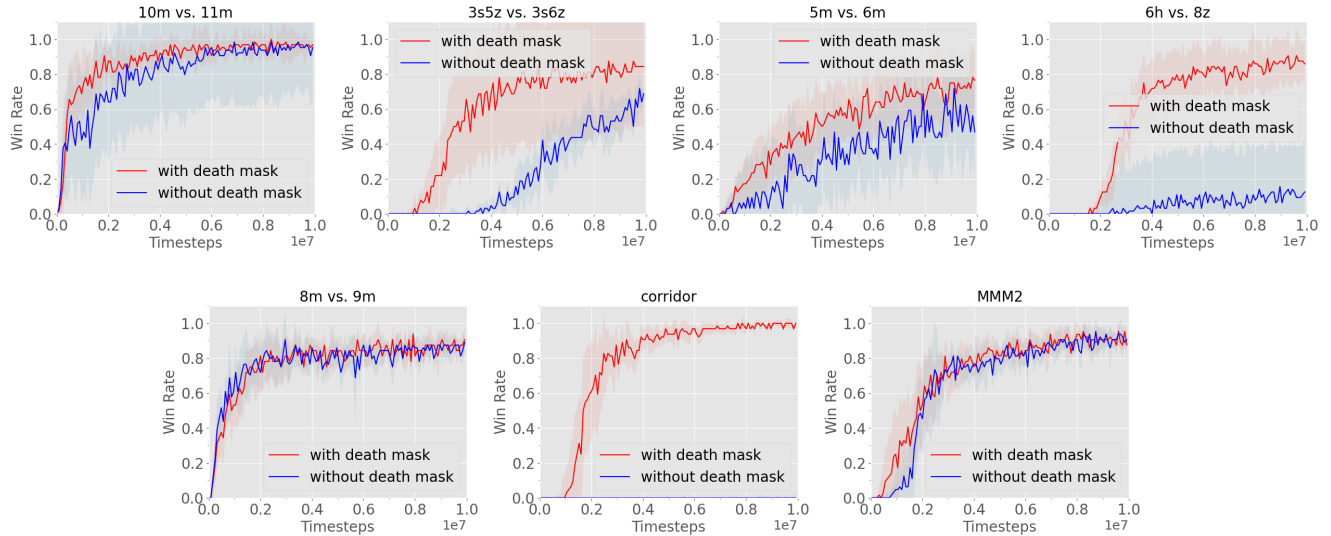


Figure 18. Ablation studies demonstrating the effect of death mask on MAPPO’s performance in the SMAC doamin.

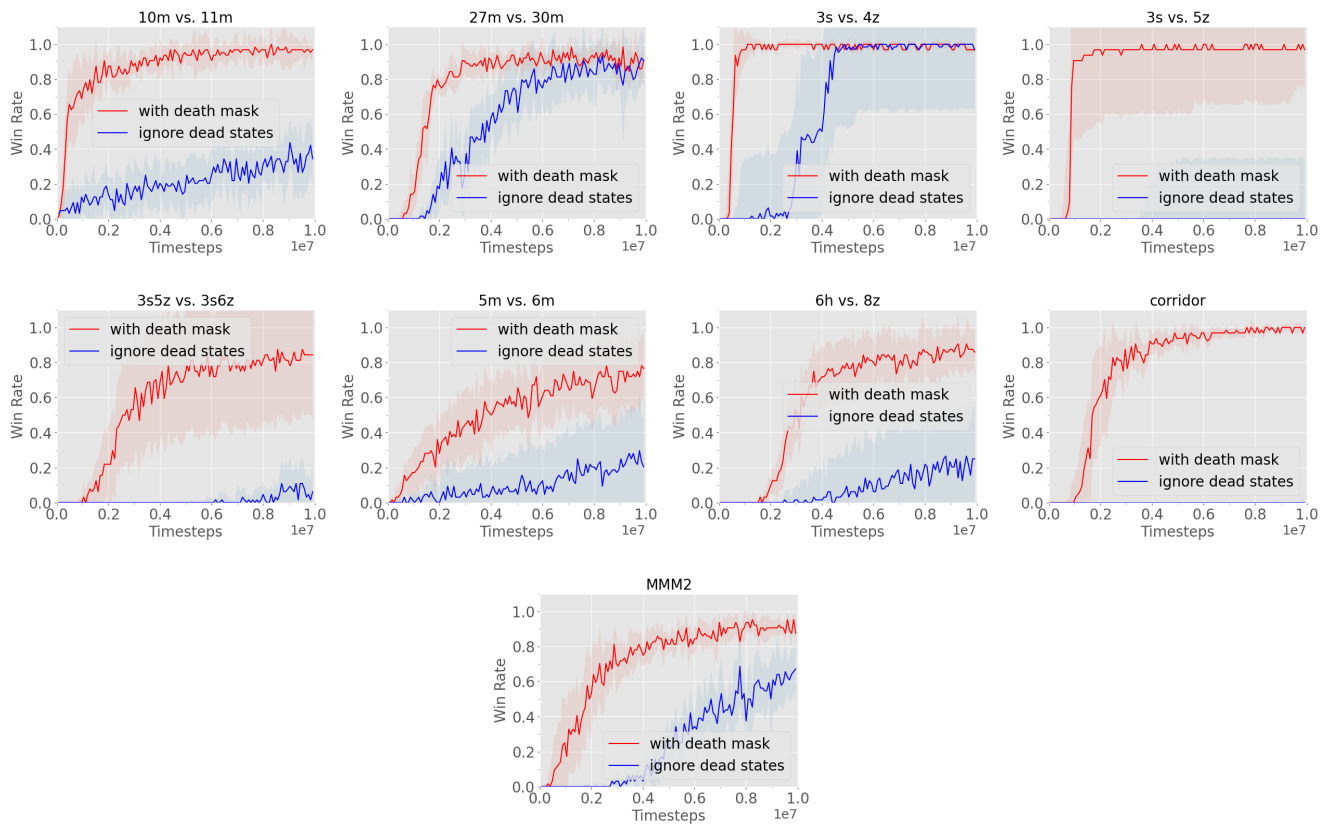


Figure 19. Ablation studies demonstrating the effect of death mask on MAPPO’s performance in the SMAC domain.

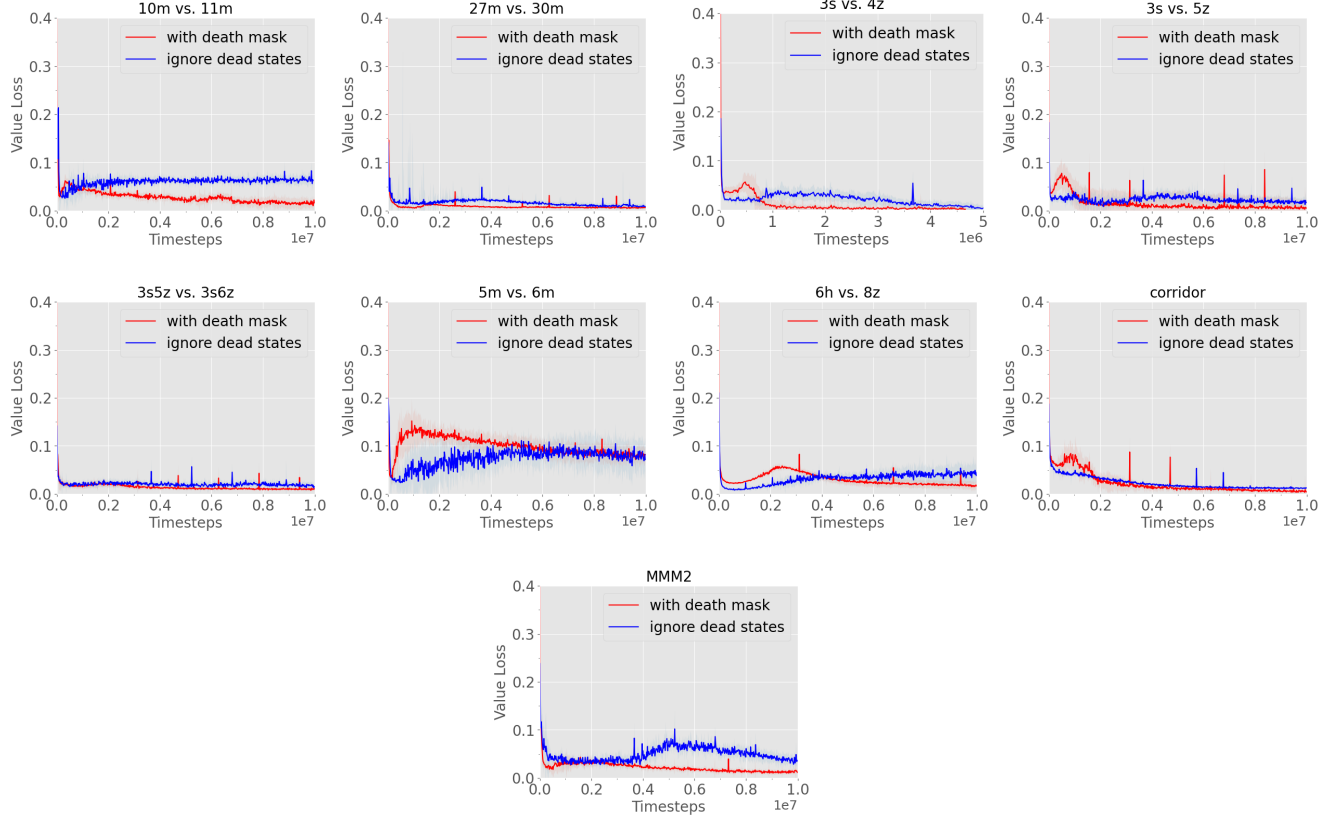


Figure 20. Effect of death mask on MAPPO’s value loss in the SMAC domain.

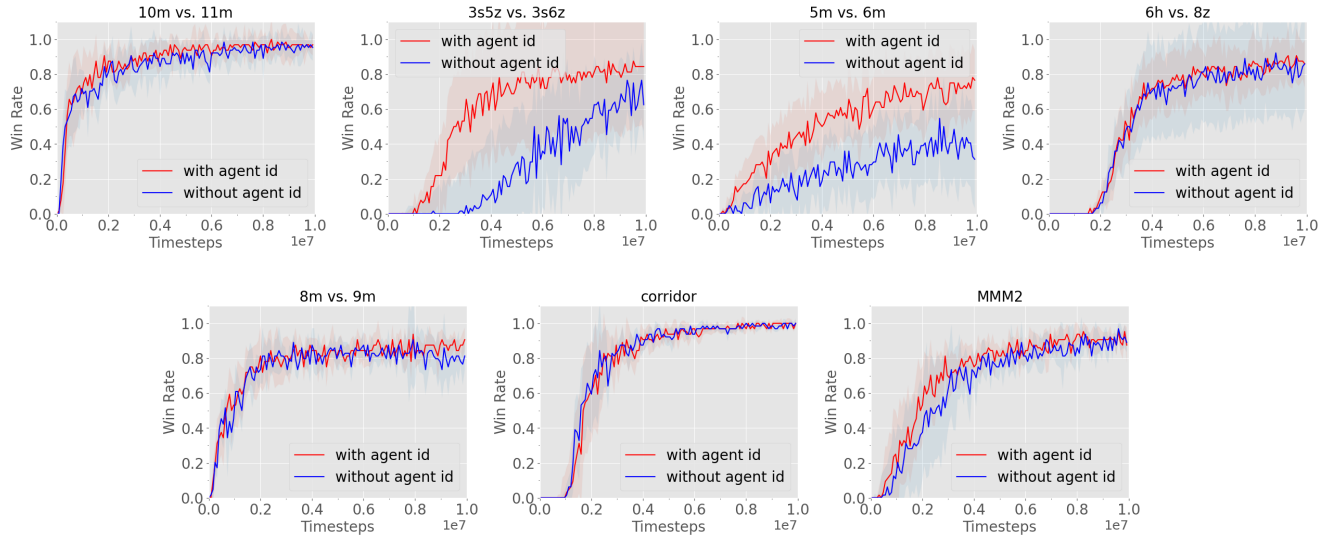


Figure 21. Ablation studies demonstrating the effect of agent id on MAPPO’s performance in the SMAC domain.